

Review

Open Access



Organic cage-based frameworks: from synthesis to applications

Jing-Wang Cui^{1,#}, Jing-Hua Yang^{1,#}, Jian-Ke Sun^{1,2,*}

¹MOE Key Laboratory of Cluster Science, Beijing Key Laboratory of Photoelectronic/Electrophotonic Conversion Materials, School of Chemistry and Chemical Engineering, Beijing Institute of Technology (Liangxiang Campus), Beijing 102488, China.

²Fujian Institute of Research on the Structure of Matter, Chinese Academy of Science, Fuzhou 350002, Fujian, China.

[#]Authors contributed equally.

* **Correspondence to:** Prof. Jian-Ke Sun, MOE Key Laboratory of Cluster Science, Beijing Key Laboratory of Photoelectronic/Electrophotonic Conversion Materials, School of Chemistry and Chemical Engineering, Beijing Institute of Technology (Liangxiang Campus), No. 8 Liangxiang East Road Fangshan District, Beijing 102488, China. E-mail: jiankesun@bit.edu.cn

How to cite this article: Cui JW, Yang JH, Sun JK. Organic cage-based frameworks: from synthesis to applications. *Chem Synth* 2024;4:30. <https://dx.doi.org/10.20517/cs.2024.01>

Received: 2 Jan 2024 **First Decision:** 25 Apr 2024 **Revised:** 15 May 2024 **Accepted:** 24 May 2024 **Published:** 4 Jun 2024

Academic Editor: Ren-Hua Jin **Copy Editor:** Pei-Yun Wang **Production Editor:** Pei-Yun Wang

Abstract

The investigation of organic cage-based frameworks (OCFs) has attracted increasing attention over the past decade due to their versatile synthetic methods and broad property range resulting from the unique combination of porous organic cages (POCs) with diverse framework materials, including porous organic polymers (POPs), metal-organic frameworks (MOFs), and supramolecular organic frameworks (SOFs). Nevertheless, a comprehensive summary of the research advancements in OCFs remains elusive in the literature. This review addresses this gap by providing a detailed overview of the development of OCF-based materials from both synthetic and applicative perspectives. The discussion begins with systematically exploring design principles and common strategies for elaborating OCFs, achieved by rational selection of bond-forming routes suitable for various POC monomers, including covalent bonds, coordination bonds, and supramolecular interactions. Subsequently, the review highlights the functional attributes derived from the distinctive structural features of OCFs, showcasing their task-specific applications in adsorption/separation, catalysis, membrane technology, and other fields. Lastly, the article summarizes the opportunities and challenges anticipated as the exploration of the OCF family continues to advance in material science.

Keywords: Porous organic cages, porous frameworks, material synthesis, applications



© The Author(s) 2024. **Open Access** This article is licensed under a Creative Commons Attribution 4.0 International License (<https://creativecommons.org/licenses/by/4.0/>), which permits unrestricted use, sharing, adaptation, distribution and reproduction in any medium or format, for any purpose, even commercially, as long as you give appropriate credit to the original author(s) and the source, provide a link to the Creative Commons license, and indicate if changes were made.



INTRODUCTION

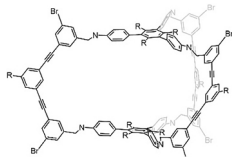
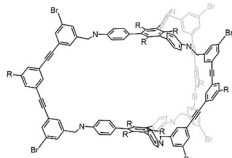
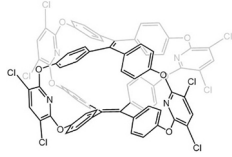
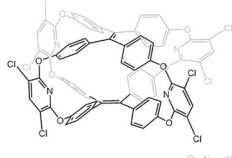
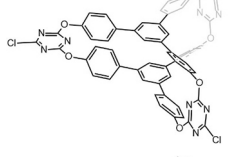
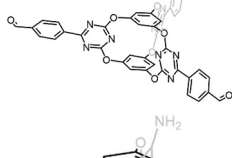
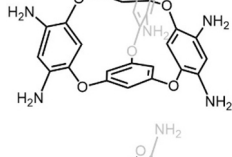
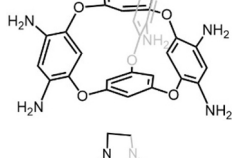
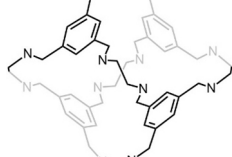
Porous organic cages (POCs) constructed by covalent bonds have emerged as novel porous materials possessing inherent permanent voids for encapsulating guest species^[1-5]. They have found applications across diverse fields ranging from adsorption/separation to molecular recognition, membrane/film technology, and catalysis^[6-12]. However, the extrinsic pore channels formed in crystalline POCs are prone to collapse upon solvent removal, which inevitably results in nonporous structures^[13]. Notably, various research teams, such as Jiang *et al.* and Song *et al.*, have made significant efforts to address this issue. They proposed amorphous scrambled POCs (ASPOCs) with enhanced porosity in the solid phase^[14,15], while in this case, effective mass transfer could be severely impeded owing to the inefficient packing of POCs. Moreover, good solubility, a unique characteristic of POCs, will, in turn, be adverse to POC recycling in specific applications. On the other hand, porous framework materials, such as porous organic polymers (POPs)^[16-19], covalent organic frameworks (COFs)^[20-24], metal-organic frameworks (MOFs)^[25-28], and supramolecular organic frameworks (SOFs)^[29-32], have attracted the attention of researchers due to their large surface area, adjustable porosity, outstanding robustness, and facile post-modification. Hence, the marriage of POCs and framework materials might give rise to task-specific organic cage-based frameworks (OCFs) with fascinating structures and exceptional performance, which not only overcome the defects of POCs but also inherit the merits of various framework materials. For instance, Ma *et al.* achieved the hierarchical construction of POC-based COFs^[33]. The interconnected channels in these frameworks enhance porosity, resulting in superior CO₂ adsorption compared to its corresponding cage precursor.

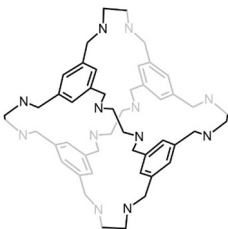
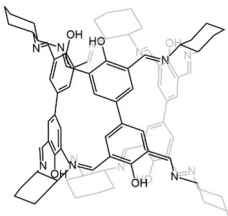
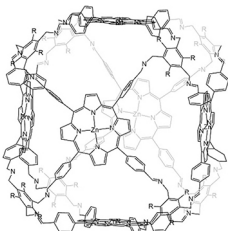
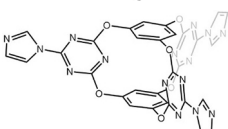
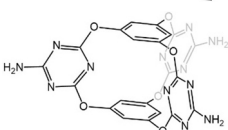
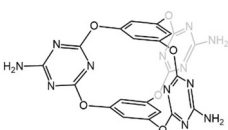
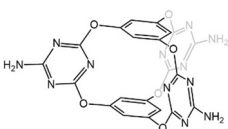
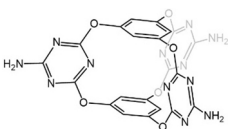
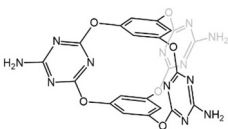
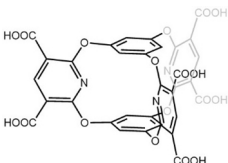
In fact, POCs are regarded as highly promising building blocks for OCFs for several reasons: (i) their good solubility^[34] enables the construction of OCFs through various synthetic reactions; (ii) their easy modification allows the introduction of functional groups^[35], facilitating the potential construction of task-specific OCFs; (iii) the combination of the intrinsic cavity in POCs with extrinsic porosity in frameworks results in the hierarchically porous structures, providing a solution to mass transfer issues; (iv) POCs, viewed as polyhedrons possessing highly connected sites, serve as excellent candidates to fabricate OCFs with charming and interesting topologies; and (v) the customizable structure of POCs provides a platform for precisely regulating the configuration of OCFs, which is beneficial for understanding the structure-property relationship. Hitherto, significant progress has been made by several groups in exploring synthetic strategies of OCFs together with the corresponding properties and applications. However, to our knowledge, no in-depth reviews have been reported on this topic. Accordingly, this review comprehensively summarized the advances of OCFs in design strategies and applications. We discussed the detailed synthetic approaches to OCFs based on various bond reactions, e.g., the covalent bond linkages, the coordination bond linkages, and the supramolecular interactions. Next, the current development of OCFs applied in materials research, including adsorption/separation, catalysis, sensing, drug delivery, actuation, and proton conductivity, is presented, followed by a brief conclusion and perspectives. A summary of the POCs used in this review is given in [Table 1](#).

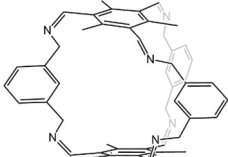
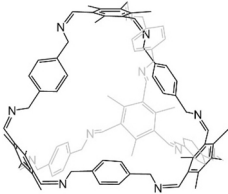
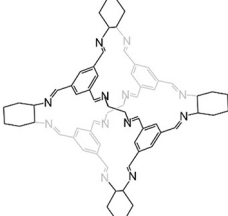
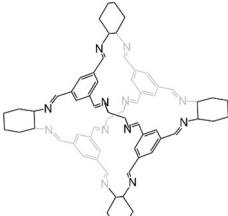
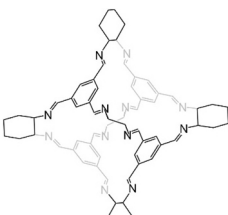
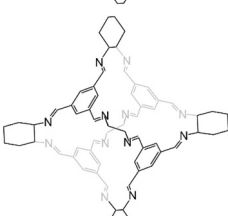
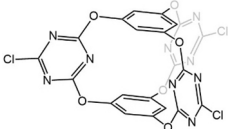

SYNTHETIC STRATEGIES

Since the introduction of the “cage-to-framework” concept in 2011, aimed at integrating the functionalities of 0D building blocks into the frameworks^[36], OCFs have been furnished in various application fields, such as gas adsorption, membrane separation, catalysis, and others. Given the tunable structural functionality and excellent solubility of POCs^[34,35], selecting appropriate bond-forming routes is crucial for constructing target frameworks. There are two primary design strategies for OCFs: (i) applying POCs as building blocks to knit tailored organic porous materials, and (ii) embedding host cages into the open framework, resulting in a so-called “host-in-host” structure. In this context, we intend to classify the synthetic approach of OCFs into three categories based on the different bond reactions involved, e.g., the covalent bond linkages, the

Table 1. Summary of POCs adopted in this review for the construction of OCFs

POCs	Structure of POCs	OCFs	Synthetic methods for OCFs	Application of OCFs	Ref.
POC-1		OCF-1	Sonogashira coupling	CO ₂ adsorption	[36]
POC-1		OCF-2 OCF-3 OCF-4	Sonogashira coupling	CO ₂ adsorption	[39]
POC-2		OCF-5	Ullmann crosscoupling	CO ₂ adsorption	[40]
POC-2		OCF-6 OCF-7	Ullmann crosscoupling	CO ₂ adsorption	[41]
POC-3		OCF-8 OCF-9 OCF-10	Nucleophilic substitution	CO ₂ adsorption	[42]
POC-4		OCF-14 OCF-15	Imine condensation	CO ₂ adsorption	[33]
POC-5		OCF-16	Imine condensation	CO ₂ adsorption	[50]
POC-5		OCF-17 OCF-18 OCF-19	Imine condensation	CO ₂ adsorption	[51]
POC-6		OCF-20	Metal coordination	-	[52]

POC-6		OCF-12 OCF-13	Interfacial crosslinking	CO ₂ separation	[44]
POC-7		OCF-21	Metal coordination	CO ₂ adsorption	[53]
POC-8		OCF-22	Metal coordination	Photocatalysis	[56]
POC-9		OCF-23 OCF-24	Metal coordination	CO ₂ adsorption	[57]
POC-10		OCF-25	Hydrogen bond	Thermal catalysis	[66]
POC-10		OCF-26	Hydrogen bond	-	[67]
POC-10		OCF-40 OCF-41 OCF-42	Imine condensation	I ₂ adsorption	[86]
POC-10		OCF-45	Hydrogen bond	Thermal catalysis	[96]
POC-10		OCF-47	Imine condensation	Drug delivery	[98]
POC-11		OCF-27 OCF-28 OCF-29 OCF-30 OCF-31	Hydrogen bond	-	[68]

POC-12		OCF-32 OCF-34	Halogen bond	-	[71]
POC-13		OCF-33	Halogen bond	-	[71]
POC-14		OCF-36	Supramolecular interactions	CO ₂ separation	[77]
POC-14		OCF-39	Supramolecular interactions	C ₃ H ₆ /C ₃ H ₈ separation	[83]
POC-14		OCF-43	Electrostatic crosslinking	I ₂ adsorption	[88]
POC-14		OCF-49	Supramolecular interactions	Proton conductivity	[100]
POC-15		OCF-44	Nucleophilic substitution	Dye adsorption	[91]
POC-16		OCF-48	Supramolecular interactions	Actuation	[99]

POCs: Porous organic cages; OCFs: organic cage-based frameworks.

coordination bond linkages, and the supramolecular interactions. It is worth noting that the distinct characteristics of each approach not only endow the OCFs to meet a diverse range of application requirements but also contribute to clarifying the structure-property-performance relationships of these materials at the molecular level.

Synthesis through covalent bonds

Covalent bonding, one of the central concepts of modern chemistry^[37], is commonly adopted for forming molecular organic solids^[38], particularly in the context of POCs. Similarly, chemists have widely utilized covalent chemical bonding, leveraging its stable characteristics to impart robustness to the material during the construction of OCFs. In this section, we highlight distinct representative cases, whether in the form of amorphous or crystalline structures or membranes, to estimate the features of irreversible and dynamic covalent bonds in shaping OCFs.

Synthesis through irreversible bonds

The irreversible linking chemistry refers to the formation of robust bonds, such as the C–C or C–N bond obtained from the coupling reaction and the bond arising from the nucleophilic substitution. The advantage of these irreversible bonds is that they impart the formation of porous frameworks with excellent stability. The pioneering work is credited to Jin *et al.*, who reported the first OCF in 2011^[36]. Since the organic cage POC-1 prepared through the imine/metathesis reaction possesses sufficient crosslinking sites, Jin *et al.* synthesized the crosslinked framework OCF-1 using the Sonogashira reaction between POC-1 and 1,4-diethynylbenzene [Figure 1A]. Compared to POC-1, OCF-1 was more stable in common organic solvents owing to the formation of C–C bonds. On this basis, they further improved the synthetic route using the microwave-assisted method to obtain three different OCFs (OCF-2, OCF-3, and OCF-4)^[39], which could maintain their structural integrity until 417 °C confirmed by the thermogravimetric analysis (TGA), showing improved chemical and thermal stability. Unlike the conventional heating method, the microwave irradiation optimizes the resulting framework structure, providing a new method for the OCF formation.

In addition to the C–C bond, the C–N bond is also adopted for producing the OCFs. In 2018, Wang *et al.* first reported a tricyclooxalixarene-based cage with the polymerizable groups of chlorine directed outward (POC-2). They utilized it to synthesize the POP (OCF-5) by the crosscoupling reaction [Figure 1B]^[40]. This cage-based polymeric framework with the irreversible C–N bond gave the Brunauer-Emmett-Teller (BET) specific surface area (S_{BET}) of 929 m²·g⁻¹ and a pore volume of 0.612 cm³·g⁻¹, exhibiting the enhanced CO₂ capture and sensing properties. Subsequently, in 2021, the same group intended to explore the influence of organic cages on OCFs, including structure and properties, and developed two distinct OCFs (OCF-6 and OCF-7) with the specific pore channels by utilizing the regulable characteristic of oxalixarene cages [Figure 1C]^[41]. Despite having similar framework structures, the difference in the building units in the cages successfully regulated the porous properties of OCF-6 and OCF-7. In addition, the effect of organic linkers has been discussed. The nucleophilic substitution reaction between the shape-persistent cage (POC-3) and different organic linkers yielded three porous cage frameworks (OCF-8, OCF-9, and OCF-10) with the S_{BET} ranging from 628.7 to 844.3 m²·g⁻¹ [Figure 1D]^[42], highlighting the role of linkers in controlling the performance of OCFs.

To date, membrane technology has become a research hotspot due to environmental friendliness and lower energy consumption than traditional methods. Owing to the characteristics of POCs with accessible internal void, tailored functionality, and solution processability, the free-standing membranes built from the OCFs, which demonstrate enhanced selectivity and permeability, have also been synthesized through the irreversible covalent bonds. In 2020, Zhai *et al.* synthesized the free-standing polyarylate film (OCF-11) with

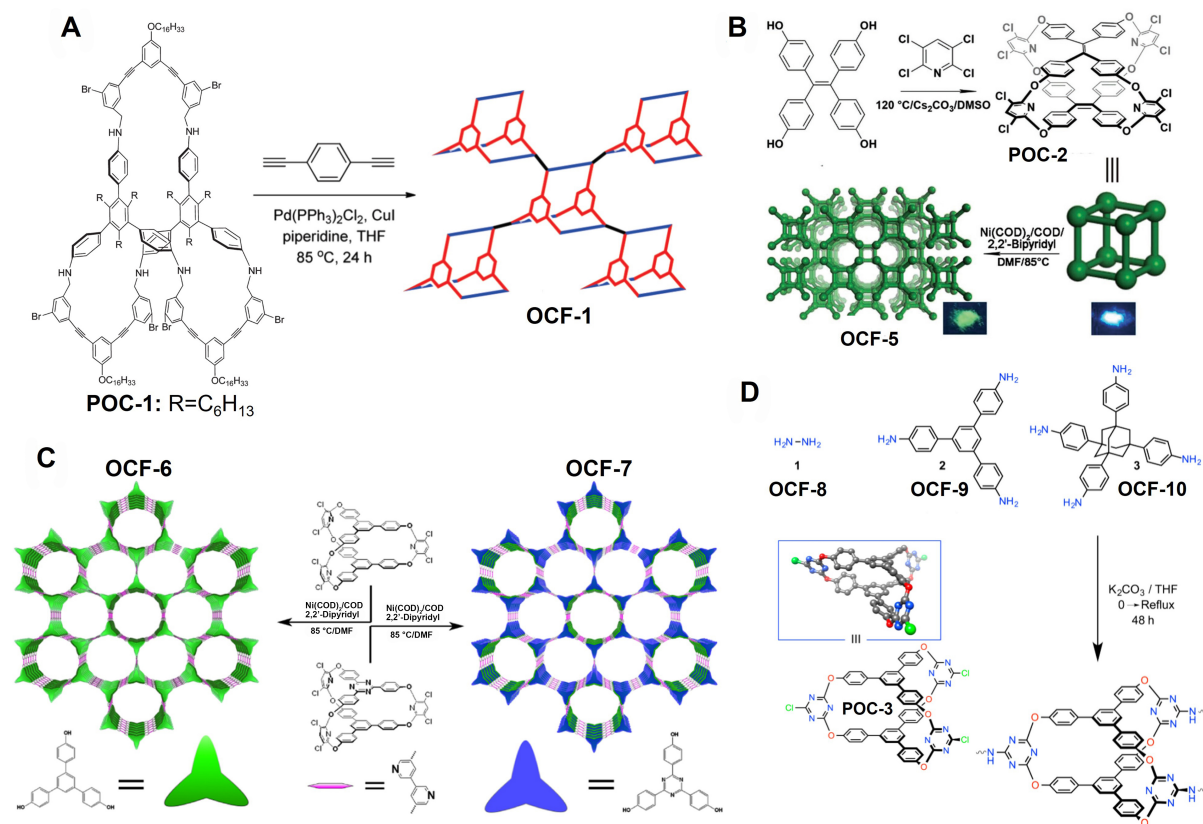


Figure 1. (A) Schematic illustration of the synthesis of **OCF-1** through the Sonogashira reaction^[36]. Copyright 2011, American Chemical Society; (B) Schematic illustration of the synthesis of **OCF-5** through the Ullmann reaction^[40]. Copyright 2018, Wiley-VCH; (C) Schematic illustration of the synthesis of **OCF-6** and **OCF-7** through the Ullmann reaction^[41]. Copyright 2021, American Chemical Society; (D) Schematic illustration of the synthesis of **OCF-8**, **OCF-9**, and **OCF-10** through the nucleophilic substitution reaction^[42]. Copyright 2015, American Chemical Society. OCF: Organic cage-based framework.

a thickness of 252 nm through the interfacial polymerization (IP) reaction^[43], wherein a kind of POC, namely Noria, in an aqueous phase could react with terephthaloyl chloride (TPC) via the formation of C–O bonds under the catalysis of triethylamine [Figure 2A]. Similarly, Jiang *et al.* utilized the IP reaction between the reduced POC (RCC3) and TPC to produce two TPC-RCC3 films (**OCF-12** and **OCF-13**)^[44]. Specifically, TPC could serve as a crosslinker, subsequently linking POC to construct a crosslinked topological network [Figure 2B].

Synthesis through dynamic bonds

COFs are crystalline porous polymers that allow the atomically precise integration of organic units into extended structures with periodic skeletons and ordered nanopores^[45–47]. Unlike amorphous porous polymers, the well-defined crystal structure of COFs provides a powerful platform to clarify the structure-property correlation and improves the relative performances^[17,48]. Accordingly, modifying the vertices of a cage to connect with other building blocks or expand its connectivity makes it an unexpected candidate for constructing COFs, particularly 3D COFs, with unique topologies. It should be noted that merging the POCs with unique physical and chemical properties could significantly enhance the functionality of resulting COFs. In this context, the dynamic covalent chemistry (DCC), especially the imine condensation, is regarded as the optimal choice for the formation of cage-based COFs, since it allows a self-correction process under thermodynamic control^[49].

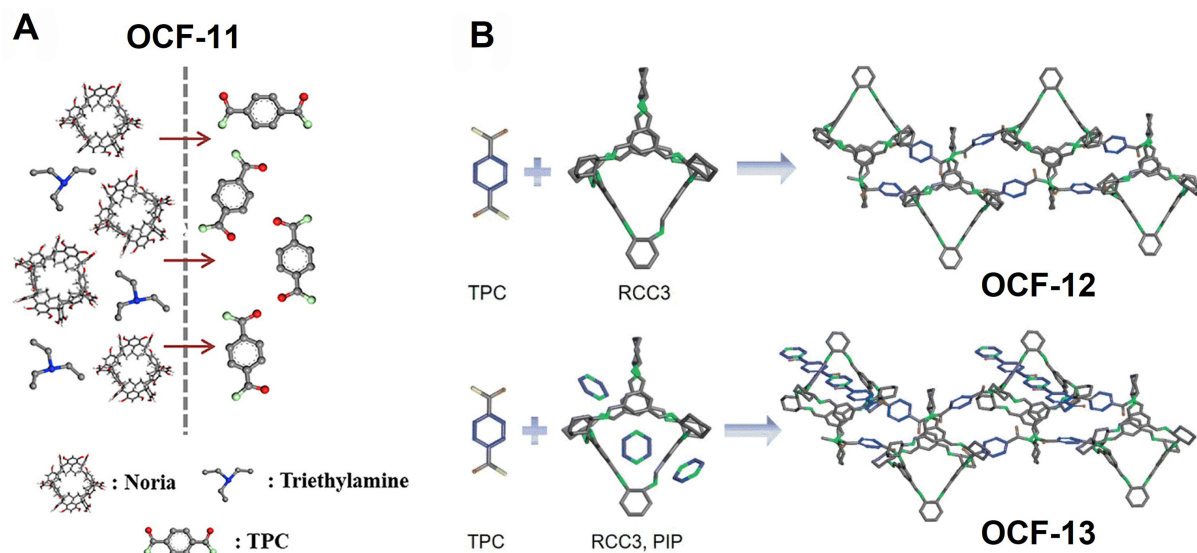


Figure 2. (A) Schematic illustration of the synthesis of polyarylate film **OCF-11** through the IP reaction^[43]. Copyright 2020, Elsevier; (B) Schematic illustration of the synthesis of **OCF-12** and **OCF-13** through the IP reaction^[44]. Copyright 2023, Royal Society of Chemistry. OCF: Organic cage-based framework; IP: interfacial polymerization.

The first two cage-based COFs were proposed by Ma *et al.* in 2019^[33]. They used a prism-like three aldehyde-containing POC (**POC-4**) to react with *p*-phenylenediamine or 4,4'-biphenyldiamine, thus obtaining two crystalline COFs, **OCF-14** and **OCF-15**, respectively [Figure 3A]. The layers of both **OCF-14** and **OCF-15** were stacked in a unique ABC mode through the π stacking of phloroglucinol faces in **POC-4**, and the crystallinities of these materials were confirmed by powder X-ray diffraction (PXRD) patterns. Notably, the ordered structure was beneficial for the CO₂ adsorption by **OCF-14** and **OCF-15**, whose values were significantly higher than that of **POC-4**. This work opens up a new direction for studying OCF materials.

Compared to 2D networks, forming 3D frameworks with novel topologies is more appealing to researchers. Zhu *et al.* reported the first cage-based 3D COF^[50]. In order to extend the dimension of the framework, a shape-persistent POC with six pendant amine groups (**POC-5**) was synthesized and chosen as the building unit. Using aniline as the modulator and acetic acid (HOAc) as the catalyst, the imine condensation between **POC-5** and 2,5-dihydroxyterephthalaldehyde (DHTPA) yielded a 3D COF (**OCF-16**) with an unreported two-fold interpenetrated *acs* topology [Figure 3B], which offered a pore volume of 0.50 cm³·g⁻¹ and S_{BET} of 1,040 m²·g⁻¹. Based on the above results, Ji *et al.* constructed three isostructural cage-based 3D COFs (**OCF-17**, **OCF-18**, and **OCF-19**) through an *in situ* acid-base neutralization strategy, aiming to investigate the method for structural regulation [Figure 3C]^[51]. By strategically pre-designing the starting dialdehyde monomers, the resulting network conformations of these three COFs could be finely tuned, which was assigned to the hinge-like motions of POC building blocks.

Synthesis through coordination bonds

Coordination bonds can reform after rupture, allowing for dynamic and reversible properties in the assembly of crystalline metal-organic hybrids. This significantly enriches the family of OCFs with explicit architecture, facilitating the elucidation of the structure-property relationship. MOFs, formed by coordination bonding between metal ions and organic ligands, constitute an extensive class of crystalline materials known for their large surface area and high pore volume. Their structural diversity and functional tunability impart MOFs with rapid developments in materials science^[25-28]. POCs, with various sites

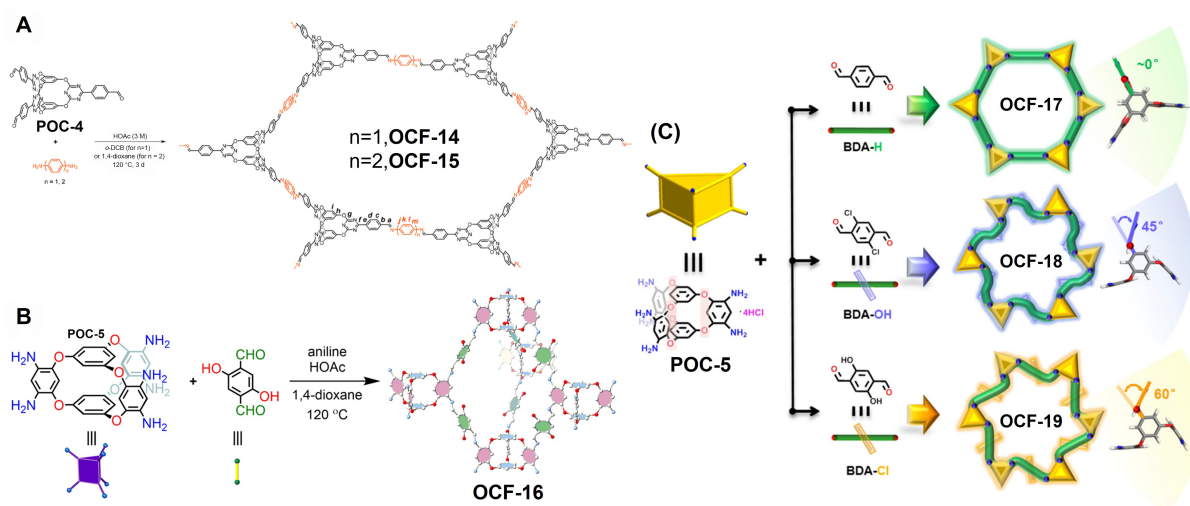


Figure 3. (A) Schematic illustration of the synthesis of **OCF-14** and **OCF-15** through the imine condensation reaction^[33]. Copyright 2019, American Chemical Society; (B) Schematic illustration of the synthesis of **OCF-16** with 3D interpenetrated structure through the imine condensation reaction^[50]. Copyright 2020, American Chemical Society; (C) Structural regulation between **OCF-17**, **OCF-18**, and **OCF-19** synthesized by an *in situ* acid-base neutralization method^[51]. Copyright 2019, Chinese Chemical Society. OCF: Organic cage-based framework.

containing lone pair electrons that can coordinate with the metal ions (such as nitrogen atoms on imine or amide bonds and oxygen atoms on hydroxyl groups), are regarded as the promising building blocks for MOF materials. Additionally, by virtue of their polyhedral shape, POCs could serve as the polyhedral building blocks to dictate the self-assembly of highly ordered hierarchical superstructures. In contrast to cage-based COFs, it is more feasible for cage-based MOFs to obtain single crystals that could be solved through the X-ray diffraction (XRD) technique to acquire accurate structures. This capability could enhance our understanding of the structure-performance relationship at the molecular level.

Swamy *et al.* not only reported the first POC but also made significant contributions to promoting the development of OCFs. In 2010, they synthesized the first cage-based MOF (**OCF-20**) by utilizing the fully reduced POC (**POC-6**) as a “preporous” ligand [Figure 4A]^[52]. Single-crystal XRD (SC-XRD) analysis revealed that **OCF-20** crystallizes in space group $F23$, comprising an octahedral arrangement of Zn(II) ions bridged by four carbonate ions in a μ_3 -fashion. The cage ligand provides six bidentate chelates to connect six neighboring Zn clusters. PXRD patterns proved that **OCF-20** could maintain its crystallinity upon heating to 100 °C under dynamic vacuum. This work demonstrates a synthetic principle for using POCs as the organic ligands and offers design inspiration for the subsequent exploitation of cage-based MOFs. Considering the flexible structures of reduced cages unsuitable for gas sorption, Zhang *et al.* developed a rigid POC (**POC-7**) that bears six terminal hydroxy groups pointing outside and utilized it as the building unit to fabricate a cage-based coordination network (**OCF-21**) with the aid of Na ions^[53]. According to the SC-XRD analysis, all the Na ions are three-coordinated with one oxygen atom and two imine nitrogen atoms from **POC-7** to construct a 1D helical chain; then, the van der Waals interactions between these neighboring helices could induce them to form a 3D coordination network with hierarchical porosity [Figure 4B]. This work emphasized that the rigid characteristic of **POC-7** contributes to forming the interconnected channels in **OCF-21**, which substantially enhanced its adsorption ability towards CO₂.

Previously, Mukhopadhyay *et al.* synthesized a shape-persistent porphyrin POC (**POC-8**) and explored its related functions^[6,54,55]. On this basis, they reported a new approach to building the cage-based MOF

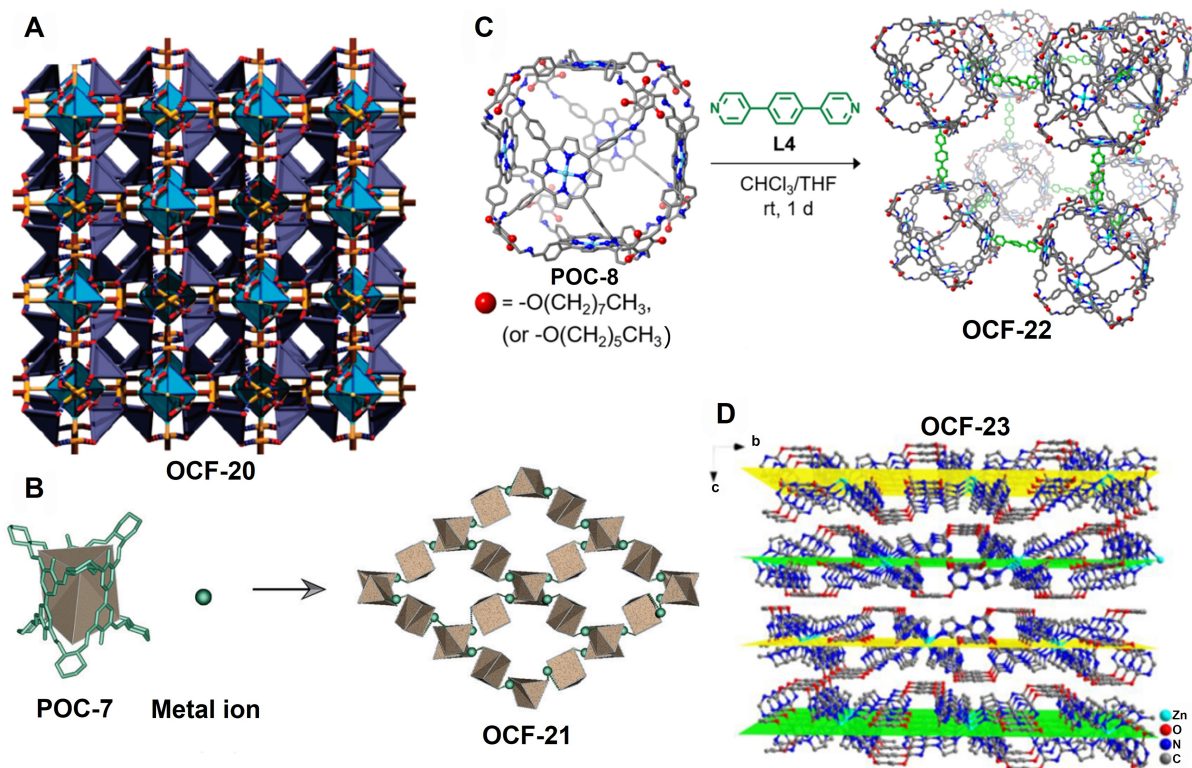


Figure 4. (A) 3D extended network structure of **OCF-20** with cubic symmetry^[52]. Copyright 2010, American Chemical Society; (B) Schematic illustration of the synthesis of **OCF-21** through the coordination bond^[53]. Copyright 2017, Wiley-VCH; (C) Schematic illustration of the synthesis of **OCF-22** through the coordination bond^[56]. Copyright 2018, American Chemical Society; (D) 2D layered structure of **OCF-23**^[57]. Copyright 2022, American Chemical Society. OCF: Organic cage-based framework.

(**OCF-22**)^[56], whose structure has been fully characterized by SC-XRD analysis [Figure 4C]. This material comprises metalated **POC-8** as the secondary building unit (SBU) and 1,4-di(4-pyridyl)-benzene as the bridging ligand. The hierarchical structure of **OCF-22** was composed of the intrinsic void from metalated **POC-8** and an extrinsic void from the 3D network. This work offers novel insights into OCFs by introducing functional cages, which might play an important role in catalysis. On the other side, the rational design and synthesis of monolayer MOFs remain great challenges. In light of this, Yang *et al.* employed an imidazole-derived POC named **POC-9** as the building block to construct two 2D cationic MOFs with isomorphic structures, abbreviated as **OCF-23** [Figure 4D] and **OCF-24**^[57]. Using **OCF-23** as the representative, it was found that the steric cage building block imparted **OCF-23** with the weak interlayer interactions estimated to be 1/46th of the graphite. Hence, the monolayer nanosheets with a thickness of 1.1 ± 0.2 nm could be exfoliated facilely on a large scale from **OCF-23** with sonication, significantly increasing physical properties.

Synthesis through supramolecular interactions

Supramolecular interactions are ubiquitous, especially in the enzyme catalysis involved in photosynthesis and metabolism, playing an irreplaceable role. Unlike covalent bonds, the soft nature of supramolecular interactions imparts materials with flexibility^[58,59], endowing them with unique properties, including processing and switchable responses to external stimuli. SOFs, assembled via the intermolecular weak non-covalent interactions (e.g., hydrogen bond, π - π stacking, electrostatic interaction, and hydrophobic association), have recently evolved into promising porous materials^[29-32]. The POCs hold promise for creating advanced SOF materials due to the following reasons: (i) the plenty of hydrogen atoms around the

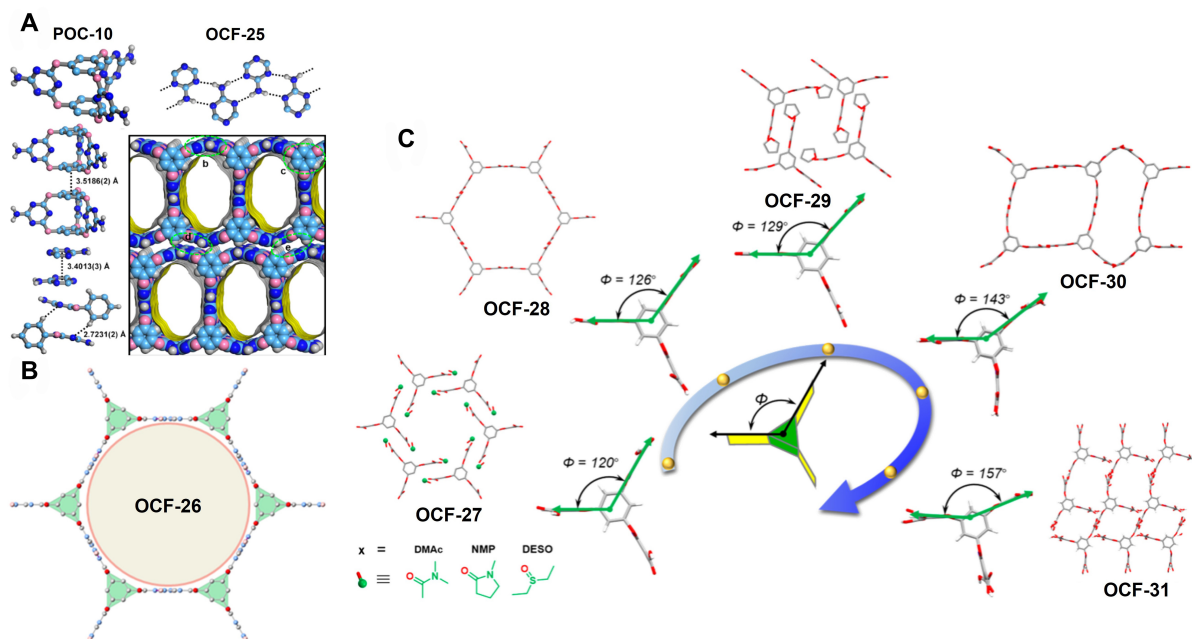


Figure 5. (A) Crystal structure of **OCF-25** synthesized through the hydrogen bond^[66]. Copyright 2019, American Chemical Society; (B) Crystal structure of **OCF-26** with hexagonal 1D channels synthesized through the hydrogen bond^[67]. Copyright 2022, American Chemical Society; (C) Structural regulation of **OCF-27** and **OCF-31** induced by hinge-like motion of **POC-11**^[68]. Copyright 2023, American Chemical Society. OCF: Organic cage-based framework.

cage skeleton provide the hydrogen bond sites; (ii) the aromatic skeleton on POCs is prone to form the effective π - π stacking interactions with other conjugated systems; (iii) the hydrophobicity of the organic cage cavity is a prerequisite for the hydrophobic association^[60]; (iv) the POCs can be charged by post-modification, facilitating the electrostatic interaction^[61].

Synthesis through hydrogen bonds

Hydrogen bonding has been a popular supramolecular tool for producing porous organic molecular crystals^[62]. As a subclass of SOFs, hydrogen-bonded organic frameworks (HOFs) are constructed by hydrogen-bonding interactions between organic building blocks^[63,64], and they are further strengthened via other weak interactions such as π - π stacking and framework interpenetration. Recent years have witnessed tremendous advances in biologically relevant applications because of their better biocompatibility^[65]. In this scenario, POCs possessing multiple hydrogen-bonding sites have the potential to function as intriguing building blocks for generating novel topological HOFs with desirable characteristics. However, this potential has not been well-explored thus far.

The first cage-based HOF (**OCF-25**) was reported by Han *et al.* in 2019^[66]; they found that the triangular prism-shaped cage, **POC-10**, produced single crystals of **OCF-25** by virtue of the slow evaporation method. The accurate structure of **OCF-25** was confirmed by SC-XRD analysis. In detail, a 2D hydrogen-bonded supramolecular network was first formed, which was further extended into a 3D porous framework with the assistance of π - π interactions [Figure 5A]. The robustness of **OCF-25** was significantly enhanced due to the multiple hydrogen bonds and π - π interactions.

The theoretical calculation is regarded as an effective tool to predict material structure. Accordingly, Zhu *et al.* discovered a cage-based HOF with the aid of computational crystal structure prediction (CSP)

calculations. Based on theoretical calculations, they synthesized the first non-interpenetrating mesoporous 3D HOF (OCF-26) through the slow diffusion method of POC-10^[67]. After characterization by SC-XRD analysis, the results showed that OCF-26 has a honeycomb shape with hexagonal 1D channels [Figure 5B]. The hierarchical character of OCF-26 resulted in a higher S_{BET} (1,750 $\text{m}^2\cdot\text{g}^{-1}$) and lower structure density (0.54 $\text{g}\cdot\text{cm}^{-3}$) than its counterpart HOF-19 (685 $\text{m}^2\cdot\text{g}^{-1}$ and 1.00 $\text{g}\cdot\text{cm}^{-3}$). Structural flexibility is one of the main characteristics of HOF materials. Recently, they also utilized a flexible oxygen-bridged prismatic POC (POC-11) decorated with six carboxylic acid groups to prepare a series of soft porous organic crystals (OCF-27 to OCF-31)^[68]. Owing to the flexible oxygen bridges in POC-11 that allow the “hinge-like” motion of trigonally arranged aromatic pillars, the different synthetic conditions endow these cage-based HOFs with diverse degrees of conformational flexibility [Figure 5C]. In addition, the structural flexibility leading to self-healing phenomena in these soft crystals has been emphasized.

Synthesis through other supramolecular interactions

In addition to hydrogen bonding, halogen bonding is a well-known highly directional non-covalent interaction that directs the self-assembly of supramolecular structures with specific functions^[69,70]. On this basis, Nieland *et al.* reported three cage-based cocrystals (OCF-32 to OCF-34) [Figure 6A]^[71], constructed using imine halogen bonding, where the imine groups of POCs (POC-12 and POC-13) serve as acceptors and polarized fluorine atoms serve as donors. Through SC-XRD analysis and theoretical calculations, the authors have proved that the halogen bonds greatly influence the formation of supramolecular OCFs.

Embedding the host cages via the electrostatic interaction into the frameworks is an appealing approach for designing OCFs. Specifically, our group proposed the unique concept of host-in-host cage composites^[72] and crafted a hierarchical self-assembly (OCF-35) through the radical co-polymerization strategy where ionic POCs were anchored into a hyper-crosslinked poly(ionic liquid) (PoPIL) owing to the electrostatic interaction [Figure 6B]. The chemical structures of OCF-35 were characterized using ¹³C cross-polarization magic-angle spinning (CP-MAS) solid-state nuclear magnetic resonance (NMR) [Figure 6C] and Fourier-transform infrared spectra (FT-IR) [Figure 6D]; meanwhile, the zeta potential measurements demonstrated that the ionic POCs were truly encapsulated in the negatively charged PoPIL shell. Superior thermal stability of up to 440 °C of the framework in OCF-35 was also found according to TGA. Micropores at 1.2 nm and mesopores ranging from 2 to 10 nm in OCF-35 with S_{BET} and a total pore volume of 410 $\text{m}^2\cdot\text{g}^{-1}$ and 0.43 $\text{cm}^3\cdot\text{g}^{-1}$, respectively, are determined by N_2 sorption isotherms at 77 K [Figure 6E]. Moreover, the porous characteristics of this cage composite could be regulated by varying the mass ratio of crosslinkers to POCs. It is suggested that this work will open up a path for OCFs with the “host-in-host” architecture in biomimetic catalysis.

In addition to the irreversible covalent bonds, supramolecular interactions are excellent candidates for manufacturing advanced separation membranes via the rational design of OCFs. POCs are regarded as the ideal filler candidates for advancing mixed matrix membranes (MMMs)^[73], owing to their enhanced affinity for the polymer matrix via weak interactions such as hydrogen bonds, π - π stacking, or hydrophobic associations^[74]. Moreover, numerous simulations have underscored the crucial role of POC fillers in MMMs^[75,76]. In this context, Bushell *et al.* pioneered a novel approach to OCF-based MMMs (OCF-36), in which the classical cage CC3 (POC-14) was combined with polymers of intrinsic microporosity (PIM) [Figure 7A]^[77]. The resulting OCF-36 exhibited superior permeability, attributed to the well-dispersed crystalline POC-14, characterized by rigidity and shape persistence. In addition, the supramolecular interactions between POC-14 and PIM enhanced the resistance of MMMs to physical aging. Building upon this foundation, Zhu *et al.* utilized the ASPOC strategy, originally proposed by Jiang *et al.*, to further enhance the separation capability of MMMs (OCF-37) by circumventing the crystallization tendency of the

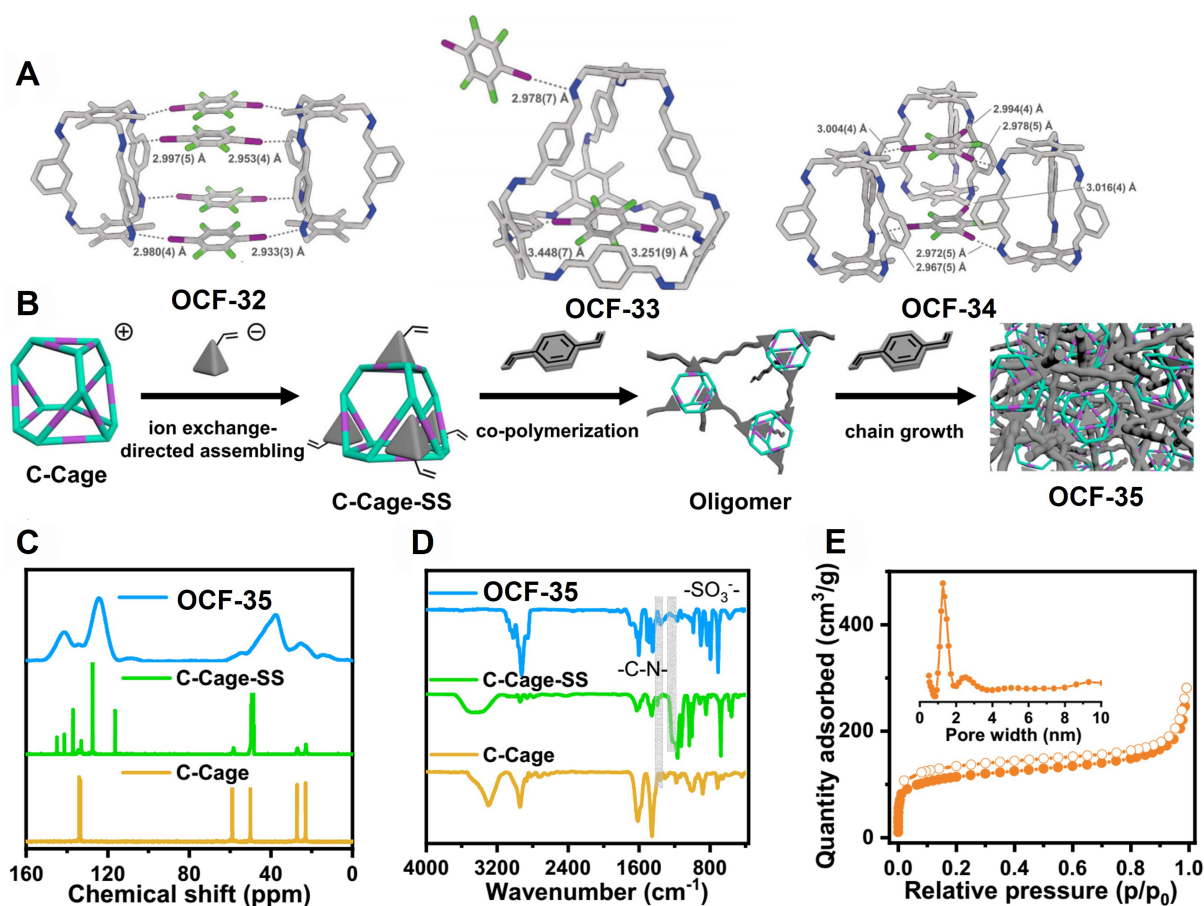


Figure 6. (A) Crystal structures of **OCF-32**, **OCF-33**, and **OCF-34** synthesized through the halogen bond^[71]. Copyright 2022, Royal Society of Chemistry; (B) Schematic illustration of the synthesis of **OCF-35** with the unique host-in-host structure through the electrostatic interaction; (C) Solid-state ¹³C CP-MAS NMR spectra of **OCF-35**; (D) FT-IR spectra of **OCF-35**; (E) N₂ sorption isotherm at 77 K and the NLDFT pore size distribution plot (inset) of **OCF-35**. (B-E) were reproduced with permission^[72]. Copyright 2022, Nature Publishing Group. OCF: Organic cage-based framework; CP-MAS: cross-polarization magic-angle spinning; NMR: nuclear magnetic resonance; FT-IR: Fourier-transform infrared spectra; NLDFT: nonlocal density functional theory.

POC molecules to realize the full integration between the filler and matrix^[14,78]. On another front, post-modification of POCs stands out as a promising avenue to enhance OCF-based MMMs. Mao *et al.* found that modifying the Noria cage to adjust weak interactions with the polyimide 4,4'-(hexafluoroisopropylidene)diphthalic anhydride-2,4,6-trimethyl-benzene-1,3-diamine (6FDA-DAM) enabled the obtained MMMs (**OCF-38**) to exhibit improved gas permeability [Figure 7B]^[79].

PROPERTIES AND APPLICATIONS

Adsorption and separation

Indeed, adsorption and separation represent pivotal industrial technologies in addressing the escalating challenges of environmental pollution and energy shortages. In this regard, POCs emerge as highly attractive adsorbents with adjustable intrinsic and extrinsic porosity, along with numerous absorption sites (e.g., oxygen and nitrogen atoms). However, the absorption capacity of these POCs is often constrained by dense packing, which not only obstructs intrinsic pores but also renders extrinsic pores ineffective. In light of this, applying the “cage-based framework” strategy offers a feasible solution for the following two reasons. First, the periodic arrangement of POCs in the cage framework enhances the accessibility of the intrinsic porosity and generates new extrinsic porosity. Second, the robust interconnection between POCs effectively prevents collapse during heat treatment.

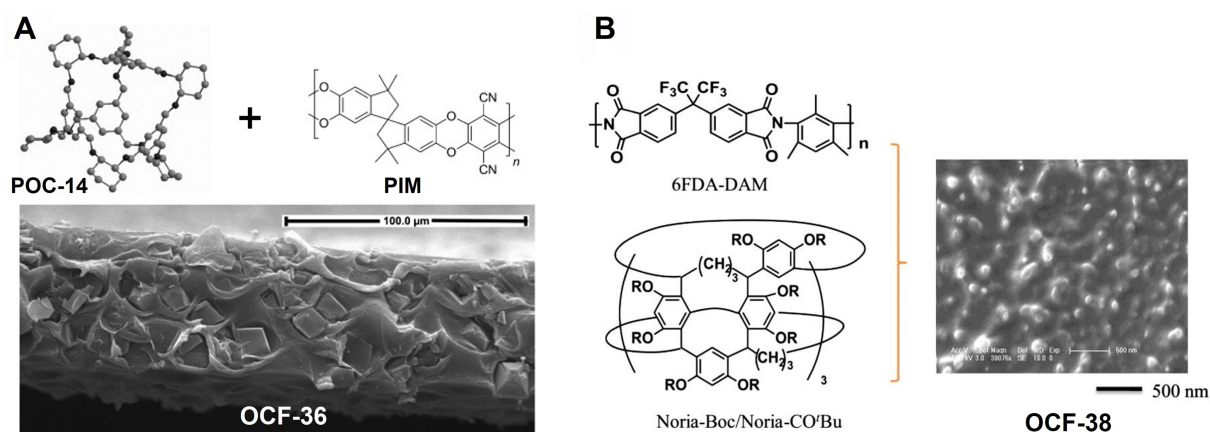


Figure 7. (A) Cross-section SEM image of **OCF-36** composed of **POC-14** and **PIM**^[77]. Copyright 2013, Wiley-VCH; (B) Cross-section SEM image of **OCF-38** composed of the modified Noria cage and the polyimide 6FDA-DAM^[79]. Copyright 2017, Elsevier. SEM: Scanning electron microscopy; OCF: organic cage-based framework; POC: porous organic cage; PIM: polymers of intrinsic microporosity; 6FDA-DAM: 4,4'-(hexafluoroisopropylidene)diphthalic anhydride-2,4,6-trimethyl-benzene-1,3-diamine.

Gas phase adsorption and separation

In order to meet the energy demand for humans, large-scale fossil fuel is combusted, which leads to massive CO₂ releasing into the atmosphere^[80]; this process disturbs the carbon balance and results in the so-called “greenhouse effect”^[81]. Given the high-efficient, low-cost, and energy-saving characteristics, CO₂ capture and storage are considered the best choices for alleviating the energy crisis and climate deterioration^[82]. So far, many OCFs have been successfully adopted in the application of CO₂ adsorption and separation.

OCF-1, as discussed above^[36], showed almost four times higher CO₂ uptake (1.22 mol·mol⁻¹) than its precursor POC-1 (0.3 mol·mol⁻¹) under standard temperature and pressure conditions, highlighting the advantage of hierarchical pores in OCFs for enhanced uptake. The enhanced adsorption ability could be attributed to the crystalline characteristics of OCFs, enabling the ordered distribution of cages. This ordered arrangement facilitates the transport of CO₂, thereby improving adsorption efficiency. Subsequently, the group investigated the gas adsorption capability of OCFs synthesized under the microwave irradiation^[39], where the adsorption capability of **OCF-2** (4.17 ± 0.02 cc·g⁻¹), **OCF-3** (5.12 ± 0.02 cc·g⁻¹), and **OCF-4** (3.64 ± 0.02 cc·g⁻¹) for the adsorption of CO₂ over N₂ could be tuned by varying the dimensional and functional features of linkers [Figure 8A]. On this basis, the critical effect of organic linkers has been further investigated by Buyukcakir *et al.* on the uptake property of OCFs towards CO₂^[42]. A comparison of **OCF-8**, **OCF-9**, and **OCF-10** at 273 K demonstrated that as the size of the organic linker increased, the uptake selectivity of CO₂ over N₂ decreased in the order of **OCF-8** (100.1) > **OCF-9** (84.7) > **OCF-10** (72.2) [Figure 8B].

It has been reported that the ordered structure of crystalline materials is more conducive to improving adsorption efficiency. Hence, the earliest reported 2D cage-based COFs were developed to capture CO₂ at 1.0 bar, with values of 43.8 cm³·g⁻¹ for **OCF-14** and 37.3 cm³·g⁻¹ for **OCF-15** at 273 K; both values are higher than those of the corresponding cage building units under the same conditions^[49]. This result demonstrated that the functional intrinsic cage cavities integrated into OCFs foster cooperative interactions for enhanced CO₂ binding. Next, researchers studied the capability of cage-based 3D COFs in higher dimensions. For example, **OCF-16**, as discussed in this review^[50], relies on its small pore size and internal cavity decorated

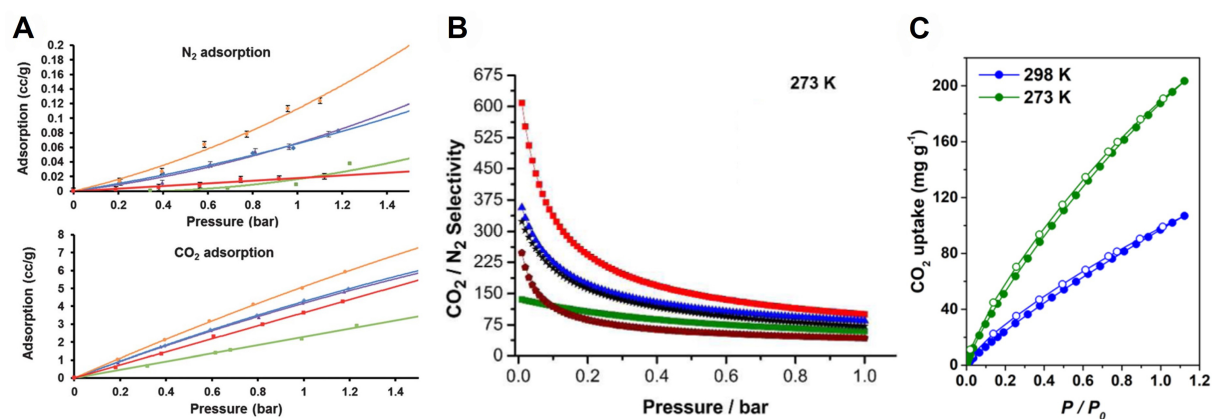


Figure 8. (A) Gas adsorption isotherms of N₂ (top) and CO₂ (bottom) for **OCF-2** (purple line), **OCF-3** (yellow line), and **OCF-4** (red line)^[39]. Copyright 2012, Royal Society of Chemistry; (B) Uptake selectivity of CO₂ over N₂ of **OCF-8** (red line), **OCF-9** (blue line), and **OCF-10** (black line)^[42]. Copyright 2015, American Chemical Society; (C) Gas adsorption isotherms of CO₂ for **OCF-16** at 273 and 298 K^[50]. Copyright 2020, American Chemical Society. OCF: Organic cage-based framework.

with nitrogen and oxygen atoms and has shown CO₂ uptake at standard temperature and pressure with a maximum of 204 mg·g⁻¹ at 273 K and 107 mg·g⁻¹ at 298 K [Figure 8C], much higher than those of 2D cage-based COFs.

In addition to the above powdered materials, membranes/films constructed from OCFs prove conducive to practical industrial implementation and have been developed for better CO₂ uptake, where the incorporated POCs play an irreplaceable role. In detail, Zhu *et al.* explored the application of OCF-based MMMs (**OCF-37**) in gas permeability^[78]. Compared to the pure Matrimid polymeric membrane, ASPOC fillers functioned as “permeability enhancers” for CO₂, resulting in a 3.4 times higher permeability of **OCF-37**. More recently, Jiang *et al.* delved into the role of crosslinkers in controlling the adsorption performance. By processing the free-standing crosslinking membrane (**OCF-12** or **OCF-13**) on the surface of a modified polysulfone (mPSf) substrate^[44], the resulting modified composite membrane, named **OCF-12/mPSf** or **OCF-13/mPSf**, was obtained. After introducing crosslinker piperazine anhydrous (PIP) for property regulation, **OCF-13/mPSf** showcased decreased permeance for CO₂ (4,303 GPU, 1 GPU = 3.35 × 10⁻¹⁰ mol·m⁻²·s⁻¹·Pa⁻¹) but an increased selectivity for CO₂/N₂ (30), in contrast to **OCF-12/mPSf** [Figure 9A]. Note that the structural characteristic of the window-to-window arrangement model of POCs is maintained in **OCF-13/mPSf**, contributing to the transport of CO₂ and thus further inducing increased gas selectivity. In addition, the extra polyamide chains in **OCF-13/mPSf** would block the external channel, thereby resulting in decreased permeance [Figure 9B]. Based on the outcomes of these case studies, OCF-based membranes hold significant potential for adsorption and separation, warranting further exploration in future research.

In addition to CO₂, certain OCFs have been employed to separate other industrial gases, such as C₃H₆/C₃H₈. In 2020, Zhang *et al.* developed a series of flexible MMMs (**OCF-39**)^[83] using POC-14 as the filler and 6FDA-DAM^[84] as the polymeric matrix [Figure 10A]. In these MMMs, evenly distributed larger recrystallized and smaller single-cage crystals create a unique hierarchical gas channel in **OCF-39**. After screening different factors influencing MMM performance (including cage loading, temperature, and pressure) [Figure 10B-D], **OCF-39** exhibited the optimal separation performance at 0.3 MPa and 20 °C, i.e., the fast C₃H₆ permeability of 396 Barrer [1 Barrer = 10⁻¹⁰ cm³ standard temperature and pressure (STP) cm/cm³·s·cm·Hg] and the good C₃H₆/C₃H₈ selectivity of 12.1. The investigation on the structure-property relationship reveals that this excellent separation ability could be due to the structural advantage of an OCF-based membrane, where the gas channels contain more adsorption sites for C₃H₆ [Figure 10E]. On the other

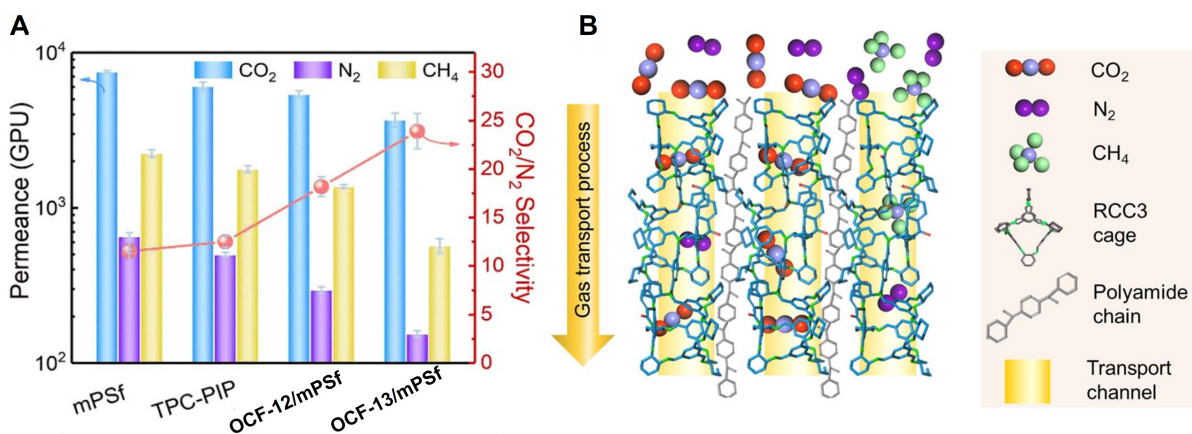


Figure 9. (A) Uptake selectivity of CO₂ over N₂ and pure CO₂, N₂, and CH₄ permeances of **OCF-12/mPsf** and **OCF-13/mPsf**; (B) Schematic illustration of the CO₂, N₂, and CH₄ transport behaviors of **OCF-13/mPsf** with gas transport channels. (A and B) were reproduced with permission^[44]. Copyright 2023, Royal Society of Chemistry. OCF: Organic cage-based framework; mPsf: modified polysulfone.

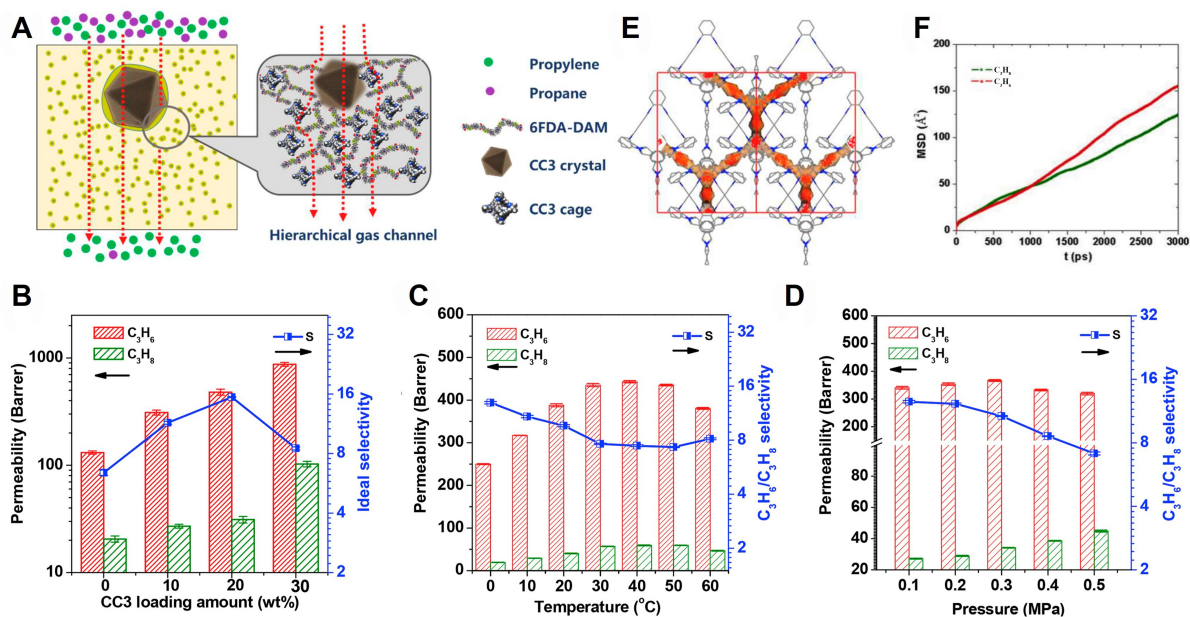


Figure 10. (A) Schematic illustration of hierarchical **OCF-39** composed of **POC-14** and the polyimide 6FDA-DAM; Effect of different factors, including cage loading (B), temperature (C), and pressure (D) on the separation performance of **OCF-39** at 0.3 MPa and 20 °C; (E) Adsorption sites of C₃H₆ in **OCF-39** calculated by the Monte Carlo simulations; (F) Radial distribution functions of C₃H₆ and C₃H₈ in **OCF-39**. (A-F) were reproduced with permission^[83]. Copyright 2020, Elsevier. OCF: Organic cage-based framework; POC: porous organic cage; 6FDA-DAM: 4,4'-(hexafluoroisopropylidene)diphthalic anhydride-2,4,6-trimethyl-benzene-1,3-diamine.

side, C₃H₆ diffuses faster than C₃H₈ because of its distinct radial distribution functions [Figure 10F].

Vigorously developing clean energy to replace fossil fuels is another strategy to mitigate the energy crisis and climate deterioration. Nuclear energy, a potential clean energy source, has received great attention from various countries because of its high energy density and lack of greenhouse gas discharge. However, the presence of radioactive iodine in nuclear waste poses a huge threat to the environment and human health^[85]. It is thus significant to remove the radioactive iodine for the safe and sustainable use of nuclear

energy. Through the electron-pair interactions between I₂ and nitrogen-rich moieties decorated in POCs, the OCFs hold the potential to adsorb iodine vapor.

Great progress for the I₂ adsorption of OCFs was made by Cheng *et al.* Recently, utilizing a nitrogen-rich POC (POC-10) as the building block, they constructed three isoreticular cage-based COFs (OCF-40 to OCF-42) by altering the linker length [Figure 11A]^[86]. The ability of these COFs to capture iodine was explored; in detail, the adsorption performance of OCF-40 (262 wt%), OCF-41 (242 wt%), and OCF-42 (131 wt%) towards iodine vapor at 77 °C under ambient pressure [Figure 11B] significantly surpassed that of POC-10 (21 wt%). The superior performance of OCF-40 could be attributed to the higher density of adsorption sites induced by the ordered cage distribution. Aiming to elucidate the adsorption mechanism, various spectral studies were performed, which demonstrated the excellent ability for iodine capture originating from the strong interaction between adsorbed iodine species and nitrogen-rich groups. During the same year, the group utilized POC-10 to synthesize four additional cage-based COFs^[87] and developed them as effective adsorbents for capturing iodine vapor.

Although the great potential of OCFs for adsorbing I₂ has been described, studies on their practical application, regarded as the ultimate goal pursued in material science, remain limited. To solve this problem, we reported a hierarchically porous poly(ionic liquid)-organic cage composite membrane (OCF-43) via a two-step strategy of evaporation and electrostatic crosslinking [Figure 11C]^[88], where a gradient content distribution of POC-14 crystals [Figure 11D] was found throughout the membrane. It should be noted that the hierarchical structure of the OCF, spanning micro-meso-macroporous porosities, exhibits a two-step adsorption behavior towards I₂ vapor at 75 °C under ambient pressure [Figure 11E], thus resulting in the enhanced uptake of I₂ up to 980 mg·g⁻¹, accompanied with an obvious color change from white to black. Particularly, by utilizing the asymmetric architecture of OCF-43, it could be processed into a practical protective material with melt-blown nonwovens [Figure 11F], which displayed an excellent rejection coefficient of 99% to I₂. We hope this work will inspire the tailored design of OCF-based composite membranes with structural hierarchy and complexity for advanced applications.

Liquid phase adsorption and separation

Water is the source of life. The wastewater containing dyes, harmful ions, and heavy metals is discharged during the industrial production or human activities and has become a serious environmental challenge^[82,89]. Leveraging their internal cavity, precise subnanometer-sized windows, and water channel-forming capabilities, POCs exhibit remarkable performance in providing ultrafast water permeance and selective separation. For example, Xu *et al.* reported the CC3 membranes containing hierarchical channels^[90], where the sub-nanoscale window of CC3 provided pathways for ion transport with a flux of 1.0 mol·m⁻²·h⁻¹ and an ion selectivity (K⁺/Mg²⁺) to 10³. Accordingly, the framework materials constructed from POCs could be more competent in water treatment. Here, we discuss the excellent performance of two OCFs applied in the water treatment, including the dye separation and salt rejection.

In 2022, Li *et al.* conducted a simple solvothermal polymerization reaction between the prism-shaped POC (POC-15) and PIP to synthesize a cage-based COF (denoted as OCF-44) [Figure 12A]^[91], with the S_{BET} of 740 m²·g⁻¹ and a pore volume of 0.49 cm³·g⁻¹. As is known, malachite green (MG) is a dye widely used in the industrial production but is carcinogenic to humans^[92]. Accordingly, OCF-44 was developed as the efficient absorbent possessing both high absorption ability and strong selectivity for MG in wastewater, emphasizing the importance of its hierarchical structure composed of the ordered external channel and the microporous internal cavity with nitrogen-rich units. Particularly, in the case of the initial dye concentration of 800 mg·L⁻¹, the maximum absorption ability of 1,805 mg·g⁻¹ was realized in OCF-44 [Figure 12B], which is

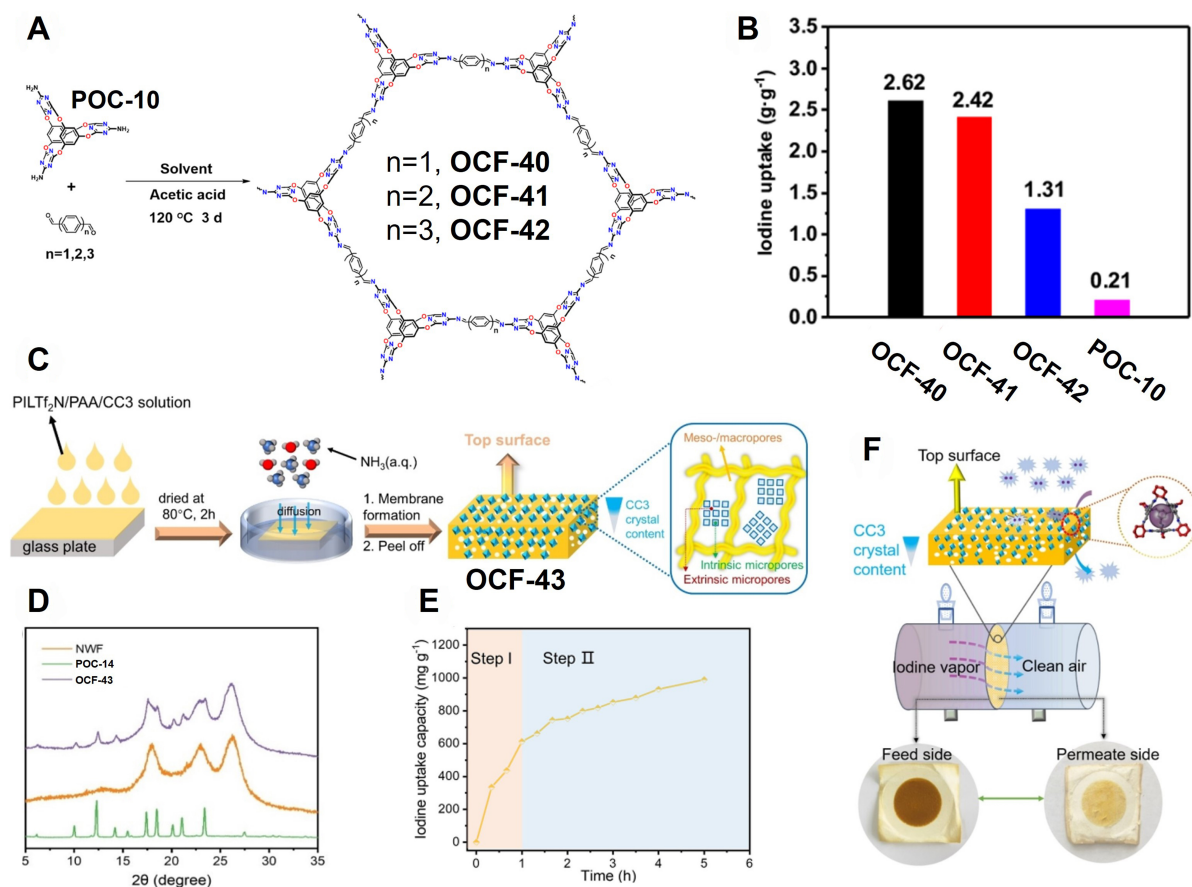


Figure 11. (A) Schematic illustration of the synthesis of **OCF-40** to **OCF-42** through the imine condensation reaction; (B) Adsorption capacity towards iodine vapor at 77 °C under ambient pressure of **OCF-40** to **OCF-42** and **POC-10**. (A and B) were reproduced with permission^[86]. Copyright 2023, American Chemical Society; (C) Schematic illustration of the synthesis of hierarchical **OCF-43** via the electrostatic crosslinking; (D) PXRD patterns of **OCF-43** and **POC-14**; (E) Time-dependent iodine vapor uptake plot of **OCF-43** at 75 °C under ambient pressure; (F) Diagram of the homemade filter device constructed from **OCF-43** for capturing iodine vapor. (C-F) were reproduced with permission^[88]. Copyright 2022, Wiley-VCH. OCF: Organic cage-based framework; POC: porous organic cage; PXRD: powder X-ray diffraction.

superior to some other absorbents including MOFs and COFs.

A film composite composed of OCFs has been used for the salt rejection. Zhai *et al.* reported the successful deposition of free-standing membrane **OCF-11** on polyacrylonitrile (PAN) support, resulting in a smooth thin-film composite (TFC)^[43]. The TFC, benefiting from the internal cavity within Noria to reduce the water transport resistance, exhibited good permeability for water. Simultaneously, according to its more densely crosslinked structure, the TFC demonstrated excellent rejection of various salts, with the rejection rate ranking in the order of $\text{Na}_2\text{SO}_4 > \text{MgSO}_4 > \text{NaCl} > \text{MgCl}_2$ [Figure 12C]. Notably, these works taking advantage of OCFs for the water treatment laid the foundation for their further application in the liquid phase adsorption/separation.

Catalysis

More recently, POCs have advanced to the excellent supports for other catalytic species, such as enzymes and nanoparticles^[93], which showcased the increased catalytic activity owing to the confinement effect of POCs. The groundbreaking research in POC-based heterogeneous catalysis began in 2015^[94]. In this study, a

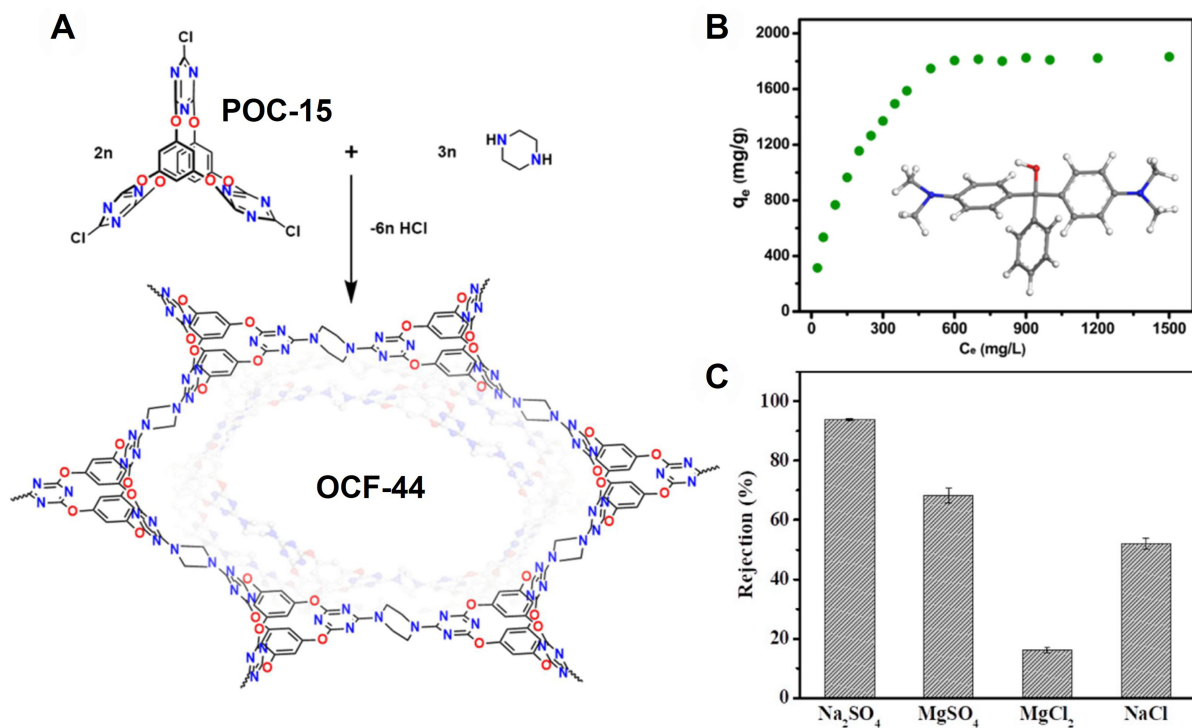


Figure 12. (A) Schematic illustration of the synthesis of **OCF-44** through the solvothermal reaction; (B) Adsorption capacity towards malachite green of **OCF-44**. (A and B) were reproduced with permission^[91]. Copyright 2022, American Chemical Society; (C) Rejection performance towards different inorganic salts of **OCF-11**^[43]. Copyright 2020, Elsevier. OCF: Organic cage-based framework.

soluble cage was utilized as a stabilizer and homogenizer to enhance the activity of heterogeneous Rh catalysts. Subsequently, alternative strategies, such as the double solvent method (DSM), have been devised to regulate the nucleation and seed growth of metal clusters (MCs) within the POC cavity^[95]. Besides, POCs themselves could also serve as supramolecular catalysts with the superior activity and specificity for their hydrophobic cavity to accumulate substrates and stabilize reaction intermediates. Accordingly, OCFs, combining the catalytic merits of POCs discussed above with the characteristics of porous frameworks, could serve as excellent candidates that surpass the role of POCs in catalytic applications, especially in heterogeneous catalysis. However, there have been fewer investigations into the application of OCFs in catalysis so far, warranting vigorous exploration in the future.

Depending on the characteristics of hierarchical pores and multiple binding sites, OCFs could be developed as excellent supports for catalysts with high loading. For instance, 3.8 wt% of the Pd ions were successfully deposited on **OCF-25**, forming the **OCF-25-Pd** composite^[66]. X-ray photoelectron spectroscopy (XPS) tests demonstrated the vital role of amino groups in binding of Pd ions to the POC precursor. The catalytic ability of **OCF-25-Pd** was evaluated using the Suzuki-Miyaura coupling reaction as a model reaction [Figure 13A]. The halogenated benzene substrates were efficiently converted into the corresponding coupling products in high yield (97) within a short time. Similarly, the cage-based HOF (**OCF-45**) constructed by using **POC-10** was used to encapsulate Ru clusters (named **OCF-45-Ru**) with a diameter of about 0.47 nm and a high loading of 30 wt%^[96]. Owing to the hydrogen bonding interactions, the **OCF-45-Ru** could dissolve into some solvents with hydrogen bonds, such as water, formic acid, and methanol, without aggregation. However, in solvents lacking hydrogen bonds, such as acetone, it precipitated. Exploiting this unique characteristic, the catalytic ability of **OCF-45-Ru** was measured via the selective

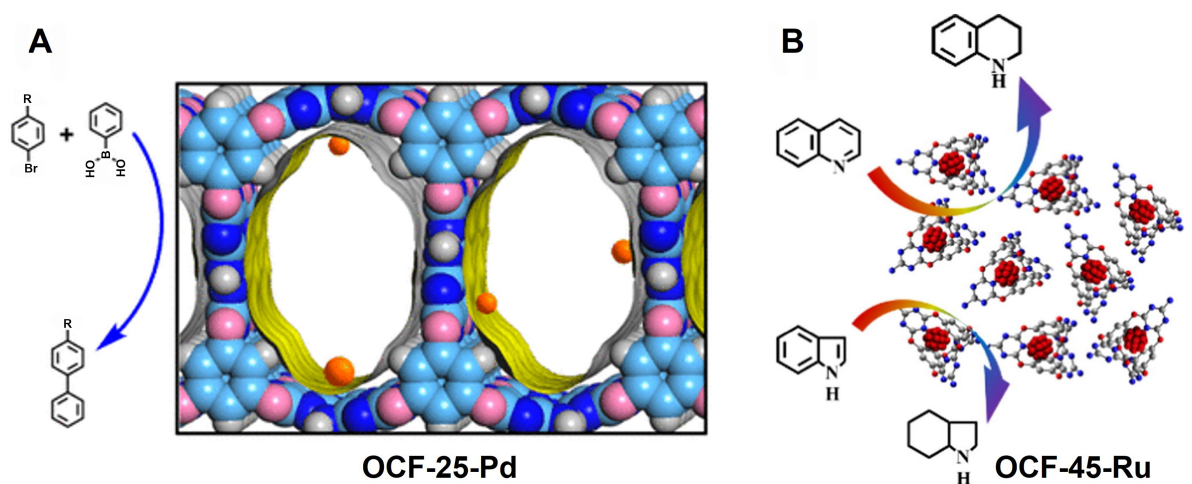


Figure 13. (A) Schematic illustration of **OCF-25-Pd** for catalyzing the Suzuki-Miyaura coupling reaction^[66]. Copyright 2019, American Chemical Society; (B) Schematic illustration of **OCF-45-Ru** for catalyzing the selective hydrogenation of quinoline derivatives^[96]. Copyright 2022, Elsevier. OCF: Organic cage-based framework.

hydrogen of quinoline derivatives [Figure 13B]. Its good solubility in the water caused the catalyst to disperse well in the form of discrete cage-confined Ru clusters, resulting in outstanding homogeneous catalytic performance towards hydrogenation of various quinoline derivatives (at least 98 conversion). Impressively, the catalyst could be precipitated from the reaction system after addition of acetone, proving the heterogeneous recyclability of OCF-45-Ru.

The delicate design of compartmentalization in organelles is responsible for the catalytic performance of enzymes with superior activity and specificity. Inspired by the wisdom of nature, we intended to build a sophisticated multi-site system based on the OCF template^[73]. Carrying the host-in-host composite of OCF-35 in hand, Au clusters with an average size of 0.67 ± 0.17 nm were successfully introduced into the inner host of ionic cages [Figure 14A]; therefore, the resulting dual-host catalyst, named OCF-35-Au, possessed the much higher catalytic performance (almost 24 times) than the mono-host counterpart [Figure 14B], attributed to the biomimetic substrate-sorting behavior achieved via electrostatic inter-host interplay. Accordingly, the electrostatically repulsive dual catalytic sites, including Au clusters in cationic cages and cationic ferrocene, were integrated with the aid of protective effect of the anionic PoPIL shell [Figure 14C], which could mimic the compartment within organelles to speed up the enzymatic-like cascade reaction [Figure 14D] by virtue of the so-called “substrate channeling effect”. This work represents our in-depth exploration of OCFs in biomimetic dual-site catalysis, guiding developing advanced host-in-host cage-based materials with associated functional features.

On this basis, we developed another novel method to construct the multi-site catalytic system. More recently, a cage hybrid (**OCF-46**) composed of the cationic POCs and anion coordination complexes (Prussian blue) was synthesized through the electrostatic interactions [Figure 14E]^[97]. By utilizing the confinement effect of POCs, the encapsulated Pd clusters could synergistically work with the Fe^{2+} sites of Prussian blue to achieve the sequential removal of organic pollutants [Figure 14F] and heavy metals [Figure 14G] in aqueous solution. Notably, this work holds promise for OCF hybrid materials in treating industrial wastewater.

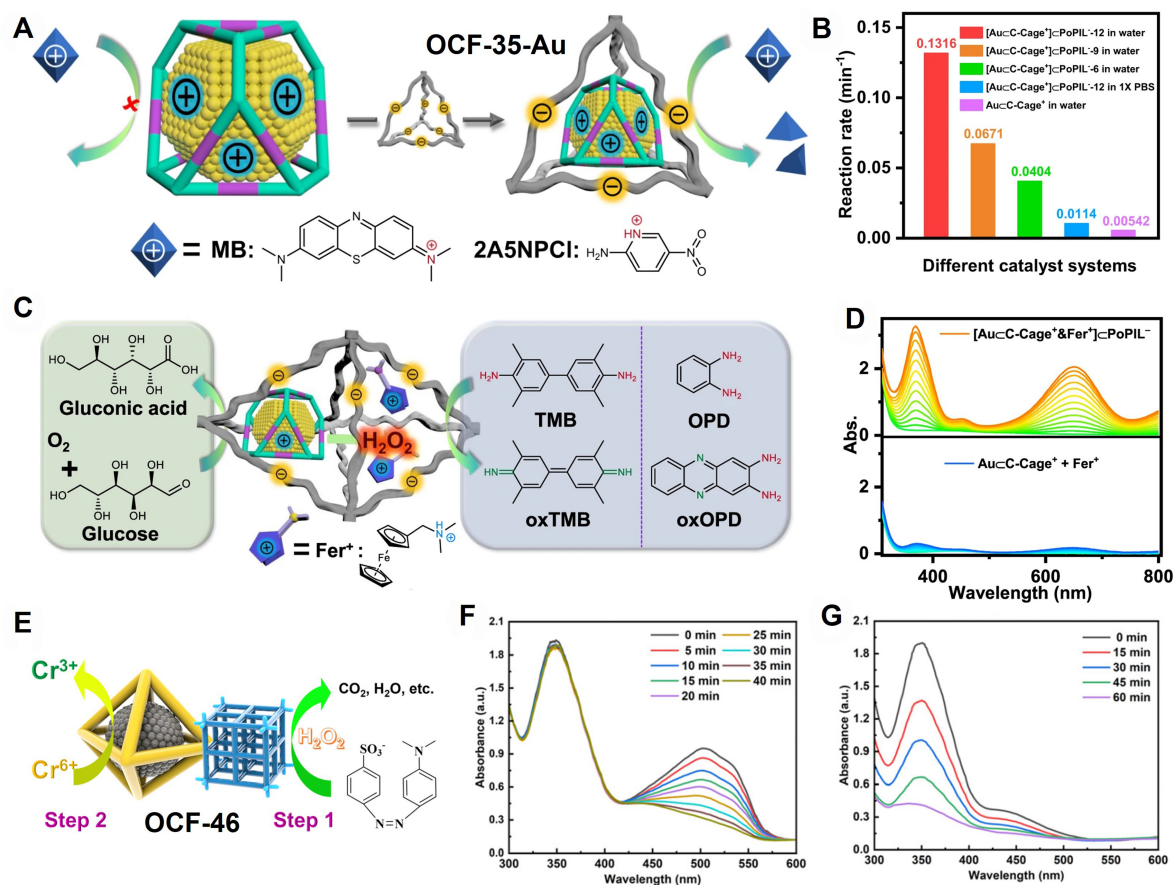


Figure 14. (A) Schematic illustration of the synthesis of **OCF-35-Au**; (B) Comparison of the reaction rate for catalytic degradation of MB by dual-host **OCF-35-Au** (red pillar) and mono-host counterpart (purple pillar); (C) Schematic illustration of the dual-site catalytic system constructed by using **OCF-35** for the cascade reaction; (D) UV-Vis spectral change for TMB oxidation cascade reaction with the aid of a dual-site catalytic system (top). (A-D) were reproduced with permission^[72]. Copyright 2022, Nature Publishing Group; (E) Schematic illustration of the dual-site catalytic system constructed by using **OCF-46** for the cascade reaction; UV-Vis spectral change for $K_2Cr_2O_7$ reduction (F) and MO degradation (G) with the aid of **OCF-46**. (E-G) were reproduced with permission^[97]. Copyright 2023, Royal Society of Chemistry. OCF: Organic cage-based framework; MB: methylene blue; UV: ultraviolet; TMB: 3,3',5,5'-tetramethylbenzidine; MO: methyl orange.

Other applications

Sensing

Leveraging the emission properties of porous polymers is considered a novel strategy for CO_2 sensing, a concept that has been extended to OCF materials. As for the organic polymer of **OCF-5**^[40], it exhibits fluorescence under ultraviolet (UV) light excitation (365 nm). Interestingly, the fluorescence intensity of **OCF-5** was found to significantly increase after capturing CO_2 in methanol at room temperature [Figure 15A]. This phenomenon can be attributed to dipole/quadrupole interactions between adsorbed CO_2 and nitrogen/oxygen atoms in the cage skeleton, preventing the rotation and vibration of phenyl rings in tetraphenylethylene (TPE) units. By contrast, N_2 uptake did not induce a fluorescence change under the same conditions [Figure 15B], highlighting the specificity of **OCF-5** for CO_2 sensing.

Drug delivery

In 2021, Li *et al.* developed a cage-based COF as a potent carrier for delivering drugs, including for drug loading and release^[98]. This cage-based COF, denoted as **OCF-47**, was constructed by the solvothermal reaction between POC-10 and terephthalaldehyde with the S_{BET} of $672\text{ m}^2\cdot\text{g}^{-1}$ and a pore volume of

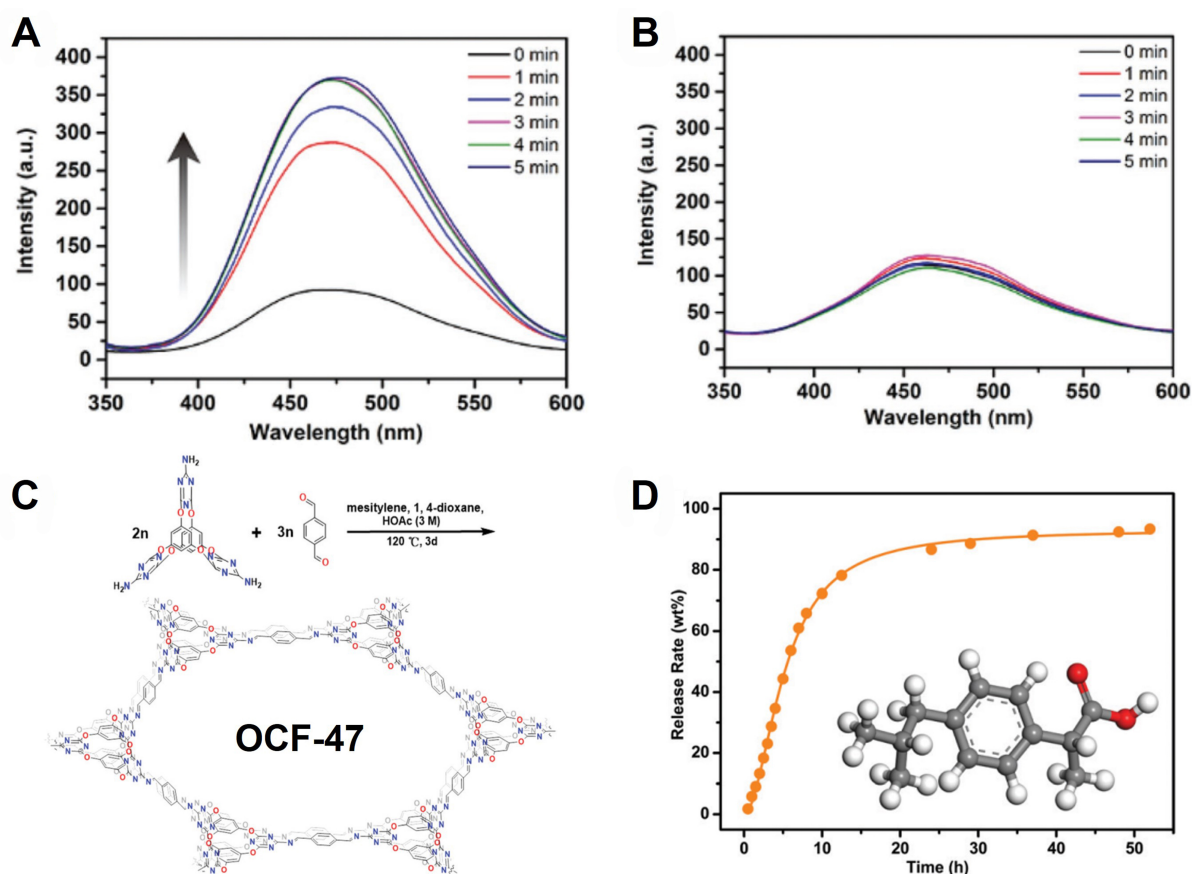


Figure 15. Change of fluorescence intensity of **OCF-5** caused by bubbling CO₂ (A) and N₂ (B)^[40]. Copyright 2018, Wiley-VCH; (C) Schematic illustration of the synthesis of **OCF-47** through the solvothermal reaction; (D) Time-dependent IBU release plot of **OCF-47**. (C and D) were reproduced with permission^[98]. Copyright 2021, Royal Society of Chemistry. OCF: Organic cage-based framework; IBU: ibuprofen.

0.52 cm³·g⁻¹ [Figure 15C]. Thanks to its large specific surface area, the **OCF-47**, with good biocompatibility, demonstrated an excellent capability in capturing three different drugs-ibuprofen (IBU), 5-fluorouracil (FLU), and captopril (CAP), with loading amounts of 17.7 wt%, 21.4 wt%, and 22.3 wt%, respectively. Subsequently, the material exhibited good drug release ability, releasing approximately 93% of IBU [Figure 15D], 93% of FLU, and 94% of CAP after about 52 h.

Actuation

Soft materials have gained increasing attention recently due to their smart or stimuli-responsive characteristics. In this context, Alimi *et al.* reported the crystalline POC-based MMMs (**OCF-48**) that exhibited vapor-triggered mechanical actuation performance^[99]. The preparation procedure of **OCF-48** is shown in Figure 16A, where the polymeric matrix of polyvinylidene fluoride (PVDF) was mixed with the POC (**POC-16**) at different concentrations. The reversible structural transformation of **POC-16** in the crystalline state towards various organic vapors, such as tetrahydropyran (THP), tetrahydrofuran (THF), dioxane, and ethyl acetate, was confirmed by using single crystal and PXRD measurements [Figure 16B and C]. Consequently, **OCF-48** inherited the vapor responsiveness of cage and experienced multiple reversible stretching and bending processes through the adsorption and desorption of THP vapor, which was attributed to the inhomogeneous distribution of **POC-16** between two faces of MMMs. Interestingly, this membrane was processed into a soft robot cartoon capable of sensing organic vapors [Figure 16D].

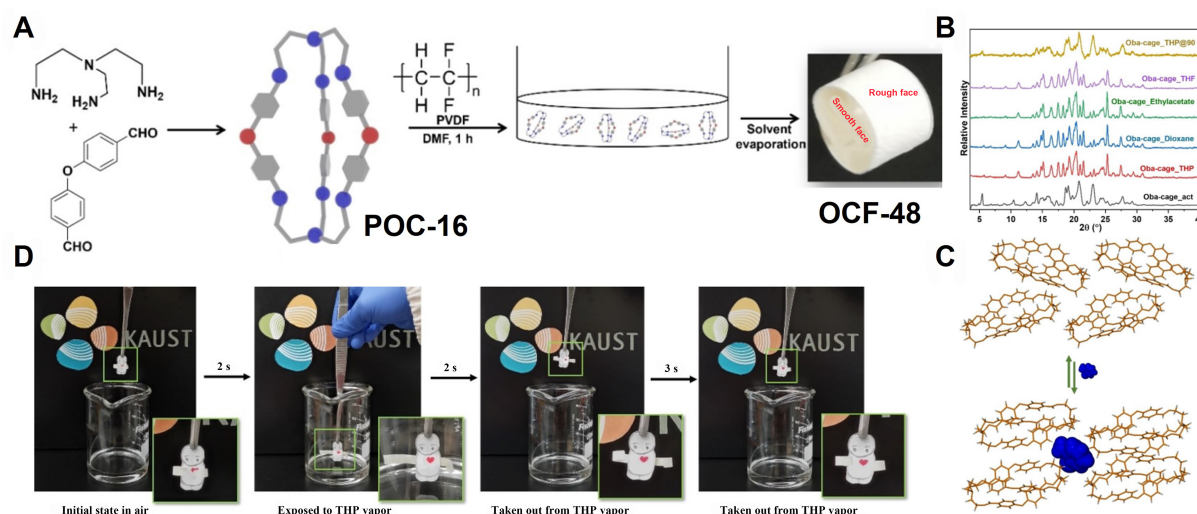


Figure 16. (A) Schematic illustration of the synthesis of **OCF-48** by mixing **POC-16** and PVDF; Single crystal (B) and powder (C) XRD measurements of **OCF-48** before and after exposure to organic vapors; (D) Open/close arm transition of the soft robot cartoon made from **OCF-48**. (A–D) were reproduced with permission^[99]. Copyright 2022, Wiley-VCH. OCF: Organic cage-based framework; POC: porous organic cage; PVDF: polyvinylidene fluoride; XRD: X-ray diffraction.

Proton conductivity

Given the high compatibility of POCs with polymer matrix, Han *et al.* mixed **POC-14** with Nafion in N,N-dimethylformamide (DMF) solvent and then obtained the MMMs, named **OCF-49** [Figure 17A]^[100]. As the mass fraction of the POCs increased from 3 to 7 wt% in the MMMs, the diffraction peaks belonging to the crystallized **POC-14** became clearer [Figure 17B], indicating the successful crystallization of organic cages in **OCF-49**. Compared to the recast Nafion, increased addition of POCs markedly improved the water retention capacity of MMMs [Figure 17C]. Hence, integrating three characteristics emerging with the formation of OCF structure, including (i) the high water absorption ability; (ii) the 3D interconnected proton channel; (iii) the hydrogen bonds formed between **POC-14** and Nafion, the excellent proton-transfer ability was found for **OCF-49**, with the optimal proton conduction of $0.085 \text{ S}\cdot\text{cm}^{-1}$ at 90°C and 40% relative humidity (RH) and $0.271 \text{ S}\cdot\text{cm}^{-1}$ at 90°C and 95% RH [Figure 17D].

CONCLUSION AND OUTLOOK

Unlike traditional porous materials, OCFs represent a new kind of framework materials characterized by a hierarchically porous structure. Over the past decade, there has been a rapid advancement in OCFs within synthetic chemistry and materials science. This is attributed to their unique advantages, including a diverse range of POC precursors and multifunctional properties for material design. Ongoing efforts are devoted to discovering the full potential of the OCF family. Different synthetic methods tailored to the structural characteristics of POCs have been developed, which successfully facilitate the transformation of POCs into diverse frameworks, such as POPs, MOFs, HOFs, SOFs, and membranes. Particularly, the distinct properties of OCF materials originating from their unique structure are discussed, e.g., excellent performance towards adsorption and separation endowed by the hierarchical porosity and pronounced catalytic ability derived from dense active sites loaded on porous frameworks. However, some crucial issues persist in the ongoing development of OCFs, necessitating attention in future research: (i) While the acceleration of POC chemistry is evident, the current repertoire of POCs reported for constructing OCFs remains limited. Extending the family of POCs in this field is desirable to introduce more diverse and intriguing functionalities into OCFs; (ii) Developing new synthetic methods closely linked to the structural diversity of materials is essential to expand the scope of OCF design. For instance, interface self-assembly

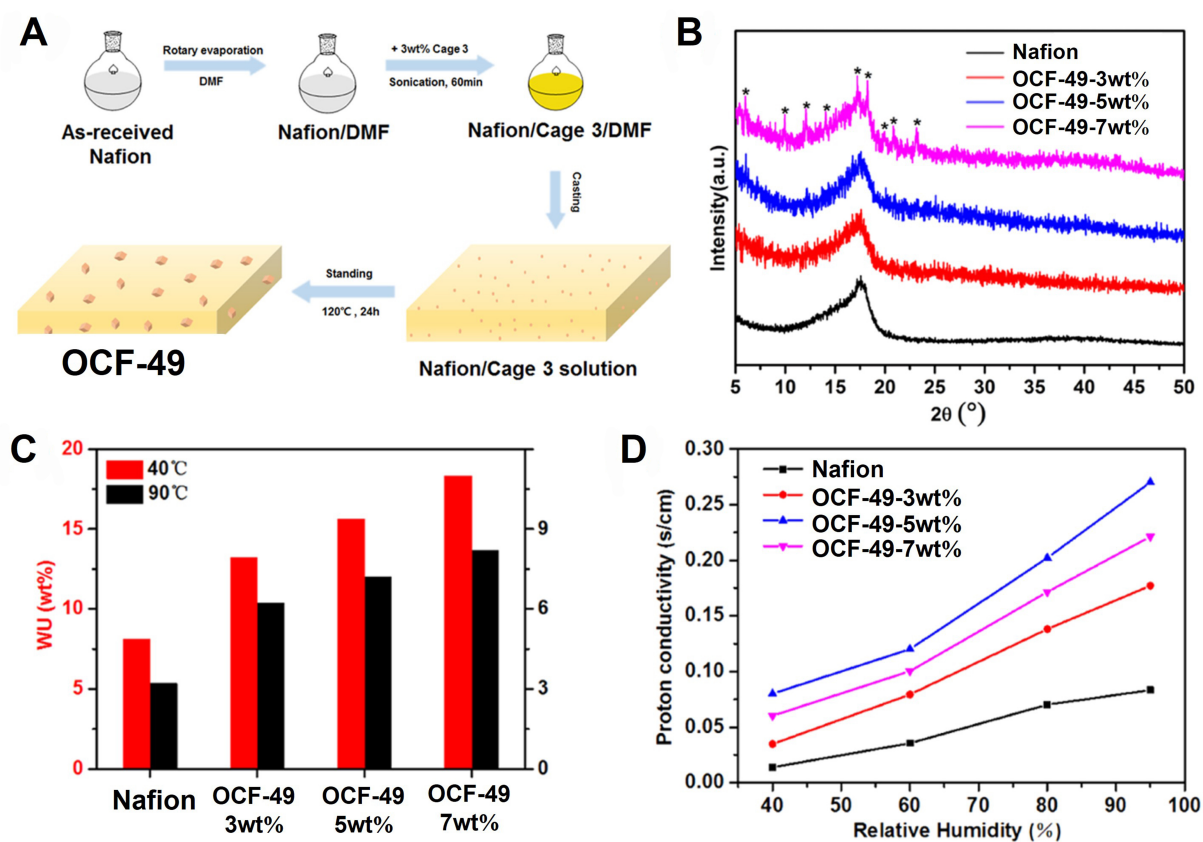


Figure 17. (A) Schematic illustration of the synthesis of **OCF-49** by mixing **POC-14** and Nafion; (B) PXRD patterns, (C) water-retention capacity, and (D) proton-transfer ability of **OCF-49** as the mass fraction of the POCs increased from 3 to 7 wt%. (A-D) were reproduced with permission^[100]. Copyright 2018, American Chemical Society. OCF: Organic cage-based framework; POC: porous organic cage; PXRD: powder X-ray diffraction.

stands out as an emerging strategy with the potential to construct ultra-thin OCF-based membranes. A recent example by our group demonstrates successful synthesis of a series of ultrathin networked cage nanofilms with a thickness of less than 8 nm^[101]. This was achieved using a universal strategy called free-interface-confined self-assembly & crosslinking (FISC) between amine cages and trimesoyl chloride. The resulting networked cage nanofilm features water channels for rapid molecular separation, with outstanding water permeability on the scale of 10^{-5} cm²·s⁻¹, surpassing that of traditional polymeric membranes by 1-2 orders of magnitude; (iii) The understanding of the relationship between structural features and performances in OCFs is still incomplete, highlighting the need to explore new materials for further clarification. In this regard, POC-based host-in-host crystalline materials warrant further exploration in the future. Such nested architectures with well-defined structural models provide an excellent platform for investigation of interhost dialogue. This may lead to the amplification of existing functions or even the creation of new properties that cannot be simply achieved by a single host alone; (iv) Presently, the application of OCFs remains in its early stages, primarily focused on adsorption and separation. A critical follow-up task is to explore broader applications of OCFs across various domains, including biomimetic catalysis, chirality recognition, photothermal conversion, and photovoltaic conversion. Emphasizing their utilization in industrial production will be particularly crucial in this exploration.

In summary, there is substantial room for exploring new structures and functions within the OCF family. This review aims to enlighten researchers about the possibilities for in-depth investigations and further advancements in this exciting field.

DECLARATIONS

Authors' contributions

Prepared the manuscript: Cui JW, Yang JH

Designed and revised the manuscript: Sun JK

Availability of data and materials

Not applicable.

Financial support and sponsorship

This work was supported by the National Natural Science Foundation of China (No. 22071008 and No. 52003029), the High-level Overseas Talents Program of China, the Excellent Young Scholars Research Fund from the Beijing Institute of Technology, the Central University Basic Research Fund of China (2021CX01024), and the Fund of State Key Laboratory of Structural Chemistry. We would like to thank the staff at the Analysis & Testing Center, Beijing Institute of Technology, for their technical support.

Conflicts of interest

All authors declared that there are no conflicts of interest.

Ethical approval and consent to participate

Not applicable.

Consent for publication

Not applicable.

Copyright

© The Author(s) 2024.

REFERENCES

1. Tozawa T, Jones JTA, Swamy SI, et al. Porous organic cages. *Nat Mater* 2009;8:973-8. [DOI](#) [PubMed](#)
2. Mastalerz M. Shape-persistent organic cage compounds by dynamic covalent bond formation. *Angew Chem Int Ed Engl* 2010;49:5042-53. [DOI](#) [PubMed](#)
3. Hasell T, Cooper AI. Porous organic cages: soluble, modular and molecular pores. *Nat Rev Mater* 2016;1:16053. [DOI](#)
4. Mastalerz M. Porous shape-persistent organic cage compounds of different size, geometry, and function. *Acc Chem Res* 2018;51:2411-22. [DOI](#) [PubMed](#)
5. Montà-González G, Sancenón F, Martínez-Mañez R, Martí-Centelles V. Purely covalent molecular cages and containers for guest encapsulation. *Chem Rev* 2022;122:13636-708. [DOI](#) [PubMed](#) [PMC](#)
6. Mukhopadhyay RD, Kim Y, Koo J, Kim K. Porphyrin boxes. *Acc Chem Res* 2018;51:2730-8. [DOI](#) [PubMed](#)
7. Liu M, Zhang L, Little MA, et al. Barely porous organic cages for hydrogen isotope separation. *Science* 2019;366:613-20. [DOI](#) [PubMed](#)
8. Acharyya K, Mukherjee PS. Organic imine cages: molecular marriage and applications. *Angew Chem Int Ed Engl* 2019;58:8640-53. [DOI](#) [PubMed](#)
9. He A, Jiang Z, Wu Y, et al. A smart and responsive crystalline porous organic cage membrane with switchable pore apertures for graded molecular sieving. *Nat Mater* 2022;21:463-70. [DOI](#) [PubMed](#) [PMC](#)
10. Hu D, Zhang J, Liu M. Recent advances in the applications of porous organic cages. *Chem Commun* 2022;58:11333-46. [DOI](#) [PubMed](#)
11. Yang X, Ullah Z, Stoddart JF, Yavuz CT. Porous organic cages. *Chem Rev* 2023;123:4602-34. [DOI](#) [PubMed](#) [PMC](#)
12. Drożdż W, Ciesielski A, Stefankiewicz AR. Dynamic cages-towards nanostructured smart materials. *Angew Chem Int Ed Engl* 2023;62:e202307552. [DOI](#) [PubMed](#)

13. Mastalerz M. Permanent porous materials from discrete organic molecules-towards ultra-high surface areas. *Chemistry* 2012;18:10082-91. DOI PubMed
14. Jiang S, Jones JTA, Hasell T, et al. Porous organic molecular solids by dynamic covalent scrambling. *Nat Commun* 2011;2:207. DOI PubMed
15. Song Q, Jiang S, Hasell T, et al. Porous organic cage thin films and molecular-sieving membranes. *Adv Mater* 2016;28:2629-37. DOI PubMed
16. McKeown NB, Budd PM. Polymers of intrinsic microporosity (PIMs): organic materials for membrane separations, heterogeneous catalysis and hydrogen storage. *Chem Soc Rev* 2006;35:675-83. DOI PubMed
17. Tan L, Tan B. Correction: Hypercrosslinked porous polymer materials: design, synthesis, and applications. *Chem Soc Rev* 2017;46:3481. DOI PubMed
18. Lee JM, Cooper AI. Advances in conjugated microporous polymers. *Chem Rev* 2020;120:2171-214. DOI PubMed PMC
19. Wang XX, Song LN, Zheng LJ, et al. Polymers with intrinsic microporosity as solid ion conductors for solid-state lithium batteries. *Angew Chem Int Ed Engl* 2023;62:e202308837. DOI PubMed
20. Zhang W, Chen L, Dai S, et al. Reconstructed covalent organic frameworks. *Nature* 2022;604:72-9. DOI PubMed PMC
21. Yang S, Lv H, Zhong H, Yuan D, Wang X, Wang R. Transformation of covalent organic frameworks from N-acylhydrazine to oxadiazole linkages for smooth electron transfer in photocatalysis. *Angew Chem Int Ed Engl* 2022;61:e202115655. DOI PubMed
22. Chen Z, Wang J, Hao M, et al. Tuning excited state electronic structure and charge transport in covalent organic frameworks for enhanced photocatalytic performance. *Nat Commun* 2023;14:1106. DOI PubMed PMC
23. Hu F, Hu Z, Liu Y, et al. Aqueous sol-gel synthesis and shaping of covalent organic frameworks. *J Am Chem Soc* 2023;145:27718-27. DOI PubMed
24. Huang N, Wang P, Jiang D. Covalent organic frameworks: a materials platform for structural and functional designs. *Nat Rev Mater* 2016;1:16068. DOI
25. Furukawa H, Cordova KE, O’Keeffe M, Yaghi OM. The chemistry and applications of metal-organic frameworks. *Science* 2013;341:1230444. DOI PubMed
26. Howarth AJ, Liu Y, Li P, et al. Chemical, thermal and mechanical stabilities of metal-organic frameworks. *Nat Rev Mater* 2016;1:15018. DOI
27. Lan G, Fan Y, Shi W, You E, Veroneau SS, Lin W. Biomimetic active sites on monolayered metal-organic frameworks for artificial photosynthesis. *Nat Catal* 2022;5:1006-18. DOI
28. Wang KY, Zhang J, Hsu YC, et al. Bioinspired framework catalysts: from enzyme immobilization to biomimetic catalysis. *Chem Rev* 2023;123:5347-420. DOI PubMed PMC
29. Lin RB, He Y, Li P, Wang H, Zhou W, Chen B. Multifunctional porous hydrogen-bonded organic framework materials. *Chem Soc Rev* 2019;48:1362-89. DOI PubMed PMC
30. Hisaki I, Suzuki Y, Gomez E, et al. Acid responsive hydrogen-bonded organic frameworks. *J Am Chem Soc* 2019;141:2111-21. DOI PubMed
31. Yuan Z, Jiang X, Chen L, et al. Sticked-layer strategy to a flexible-robust hydrogen-bonded organic framework for efficient C₂H₂/CO₂ separation. *CCS Chem* 2024;6:663-71. DOI
32. Yin Q, Alexandrov EV, Si DH, et al. Metallization-prompted robust porphyrin-based hydrogen-bonded organic frameworks for photocatalytic CO₂ reduction. *Angew Chem Int Ed Engl* 2022;61:e202115854. DOI PubMed
33. Ma JX, Li J, Chen YF, et al. Cage based crystalline covalent organic frameworks. *J Am Chem Soc* 2019;141:3843-8. DOI PubMed
34. Hasell T, Chong SY, Jelfs KE, Adams DJ, Cooper AI. Porous organic cage nanocrystals by solution mixing. *J Am Chem Soc* 2012;134:588-98. DOI PubMed
35. Wang H, Jin Y, Sun N, Zhang W, Jiang J. Post-synthetic modification of porous organic cages. *Chem Soc Rev* 2021;50:8874-86. DOI PubMed
36. Jin Y, Voss BA, Jin A, Long H, Noble RD, Zhang W. Highly CO₂-selective organic molecular cages: what determines the CO₂ selectivity. *J Am Chem Soc* 2011;133:6650-8. DOI PubMed
37. Bacskey GB, Reimers JR, Nordholm S. The mechanism of covalent bonding. *J Chem Educ* 1997;74:1494. DOI
38. Holst JR, Trewin A, Cooper AI. Porous organic molecules. *Nat Chem* 2010;2:915-20. DOI PubMed
39. Jin Y, Voss BA, Mccaffrey R, Baggett CT, Noble RD, Zhang W. Microwave-assisted syntheses of highly CO₂-selective organic cage frameworks (OCFs). *Chem Sci* 2012;3:874-7. DOI
40. Wang Z, Ma H, Zhai TL, et al. Networked cages for enhanced CO₂ capture and sensing. *Adv Sci* 2018;5:1800141. DOI PubMed PMC
41. Wang Z, Ou Q, Ma H, et al. Molecular engineering for organic cage frameworks with fixed pore size to tune their porous properties and improve CO₂ capture. *ACS Appl Polym Mater* 2021;3:171-7. DOI
42. Buyukcakir O, Seo Y, Coskun A. Thinking outside the cage: controlling the extrinsic porosity and gas uptake properties of shape-persistent molecular cages in nanoporous polymers. *Chem Mater* 2015;27:4149-55. DOI
43. Zhai Z, Jiang C, Zhao N, et al. Polyarylate membrane constructed from porous organic cage for high-performance organic solvent nanofiltration. *J Membrane Sci* 2020;595:117505. DOI
44. Jiang Z, Wang Y, Sheng M, et al. A highly permeable porous organic cage composite membrane for gas separation. *J Mater Chem A* 2023;11:6831-41. DOI

45. Côté AP, Benin AI, Ockwig NW, O’Keeffe M, Matzger AJ, Yaghi OM. Porous, crystalline, covalent organic frameworks. *Science* 2005;310:1166-70. DOI PubMed
46. Diercks CS, Yaghi OM. The atom, the molecule, and the covalent organic framework. *Science* 2017;355:eaal1585. DOI PubMed
47. Qian C, Feng L, Teo WL, et al. Imine and imine-derived linkages in two-dimensional covalent organic frameworks. *Nat Rev Chem* 2022;6:881-98. DOI PubMed
48. Wang S, Yang Y, Zhang Z. Designing and molding covalent organic frameworks for separation applications. *Acc Mater Res* 2023;4:953-67. DOI
49. Baek K, Hwang I, Roy I, Shetty D, Kim K. Self-assembly of nanostructured materials through irreversible covalent bond formation. *Acc Chem Res* 2015;48:2221-9. DOI PubMed
50. Zhu Q, Wang X, Clowes R, et al. 3D cage COFs: a dynamic three-dimensional covalent organic framework with high-connectivity organic cage nodes. *J Am Chem Soc* 2020;142:16842-8. DOI PubMed PMC
51. Ji C, Su K, Wang W, et al. Tunable cage-based three-dimensional covalent organic frameworks. *CCS Chem* 2022;4:3095-105. DOI
52. Swamy SI, Bacsá J, Jones JTA, et al. A metal-organic framework with a covalently prefabricated porous organic linker. *J Am Chem Soc* 2010;132:12773-5. DOI PubMed
53. Zhang L, Xiang L, Hang C, Liu W, Huang W, Pan Y. From discrete molecular cages to a network of cages exhibiting enhanced CO₂ adsorption capacity. *Angew Chem Int Ed Engl* 2017;56:7787-91. DOI PubMed
54. Hong S, Rohman MR, Jia J, et al. Porphyrin boxes: rationally designed porous organic cages. *Angew Chem Int Ed Engl* 2015;54:13241-4. DOI PubMed
55. Benke BP, Aich P, Kim Y, et al. Iodide-selective synthetic ion channels based on shape-persistent organic cages. *J Am Chem Soc* 2017;139:7432-5. DOI PubMed
56. Kim Y, Koo J, Hwang IC, et al. Rational design and construction of hierarchical superstructures using shape-persistent organic cages: porphyrin box-based metallosupramolecular assemblies. *J Am Chem Soc* 2018;140:14547-51. DOI PubMed
57. Yang P, Jiang J, Ma JP, et al. Monolayer nanosheets exfoliated from cage-based cationic metal-organic frameworks. *Inorg Chem* 2022;61:1521-9. DOI PubMed
58. Huang YG, Shiota Y, Wu MY, et al. Superior thermoelasticity and shape-memory nanopores in a porous supramolecular organic framework. *Nat Commun* 2016;7:11564. DOI PubMed PMC
59. Zhang G, Li B, Zhou Y, et al. Processing supramolecular framework for free interconvertible liquid separation. *Nat Commun* 2020;11:425. DOI PubMed PMC
60. Hua M, Wang S, Gong Y, Wei J, Yang Z, Sun JK. Hierarchically porous organic cages. *Angew Chem Int Ed Engl* 2021;60:12490-7. DOI PubMed
61. Zhang SY, Kochovski Z, Lee HC, et al. Ionic organic cage-encapsulating phase-transferable metal clusters. *Chem Sci* 2019;10:1450-6. DOI PubMed PMC
62. Tian J, Chen L, Zhang DW, Liu Y, Li ZT. Supramolecular organic frameworks: engineering periodicity in water through host-guest chemistry. *Chem Commun* 2016;52:6351-62. DOI PubMed
63. Li P, Ryder MR, Stoddart JF. Hydrogen-bonded organic frameworks: a rising class of porous molecular materials. *Acc Mater Res* 2020;1:77-87. DOI
64. Wang B, Lin RB, Zhang Z, Xiang S, Chen B. Hydrogen-bonded organic frameworks as a tunable platform for functional materials. *J Am Chem Soc* 2020;142:14399-416. DOI PubMed
65. Yu D, Zhang H, Ren J, Qu X. Hydrogen-bonded organic frameworks: new horizons in biomedical applications. *Chem Soc Rev* 2023;52:7504-23. DOI PubMed
66. Han B, Wang H, Wang C, et al. Postsynthetic metalation of a robust hydrogen-bonded organic framework for heterogeneous catalysis. *J Am Chem Soc* 2019;141:8737-40. DOI PubMed PMC
67. Zhu Q, Johal J, Widdowson DE, et al. Analogy powered by prediction and structural invariants: computationally led discovery of a mesoporous hydrogen-bonded organic cage crystal. *J Am Chem Soc* 2022;144:9893-901. DOI PubMed PMC
68. Zhu Q, Wei L, Zhao C, et al. Soft hydrogen-bonded organic frameworks constructed using a flexible organic cage hinge. *J Am Chem Soc* 2023;145:23352-60. DOI PubMed PMC
69. Metrangolo P, Meyer F, Pilati T, Resnati G, Terraneo G. Halogen bonding in supramolecular chemistry. *Angew Chem Int Ed Engl* 2008;47:6114-27. DOI PubMed
70. Dumele O, Trapp N, Diederich F. Halogen bonding molecular capsules. *Angew Chem Int Ed Engl* 2015;54:12339-44. DOI PubMed
71. Nieland E, Komisarek D, Hohloch S, et al. Supramolecular networks by imine halogen bonding. *Chem Commun* 2022;58:5233-6. DOI PubMed
72. Tan L, Zhou JH, Sun JK, Yuan J. Electrostatically cooperative host-in-host of metal cluster C_{60} ionic organic cages in nanopores for enhanced catalysis. *Nat Commun* 2022;13:1471. DOI PubMed PMC
73. Dechnik J, Gascon J, Doonan CJ, Janiak C, Sumbly CJ. Mixed-matrix membranes. *Angew Chem Int Ed Engl* 2017;56:9292-310. DOI PubMed
74. Chen T, Li Y, Wei Y, Zhang Y, Zhu J, Van der Bruggen B. Exploring the potential of porous organic cage membranes: recent advances and applications. *Sep Purif Technol* 2024;330:125440. DOI
75. Evans JD, Huang DM, Hill MR, Sumbly CJ, Thornton AW, Doonan CJ. Feasibility of mixed matrix membrane gas separations employing porous organic cages. *J Phys Chem C* 2014;118:1523-9. DOI

76. Kong X, Liu J. An atomistic simulation study on POC/PIM mixed-matrix membranes for gas separation. *J Phys Chem C* 2019;123:15113-21. [DOI](#)
77. Bushell AF, Budd PM, Attfield MP, et al. Nanoporous organic polymer/cage composite membranes. *Angew Chem Int Ed Engl* 2013;52:1253-6. [DOI](#) [PubMed](#) [PMC](#)
78. Zhu G, Zhang F, Rivera MP, et al. Molecularly mixed composite membranes for advanced separation processes. *Angew Chem Int Ed Engl* 2019;58:2638-43. [DOI](#) [PubMed](#)
79. Mao H, Zhang S. Mixed-matrix membranes incorporated with porous shape-persistent organic cages for gas separation. *J Colloid Interface Sci* 2017;490:29-36. [DOI](#) [PubMed](#)
80. Ding M, Flaig RW, Jiang HL, Yaghi OM. Carbon capture and conversion using metal-organic frameworks and MOF-based materials. *Chem Soc Rev* 2019;48:2783-828. [DOI](#) [PubMed](#)
81. Li J, Ma Y, Mccarthy MC, et al. Carbon dioxide capture-related gas adsorption and separation in metal-organic frameworks. *Coord Chem Rev* 2011;255:1791-823. [DOI](#)
82. Mohammed N, Lian H, Islam MS, et al. Selective adsorption and separation of organic dyes using functionalized cellulose nanocrystals. *Chem Eng J* 2021;417:129237. [DOI](#)
83. Zhang Q, Li H, Chen S, Duan J, Jin W. Mixed-matrix membranes with soluble porous organic molecular cage for highly efficient C₃H₆/C₃H₈ separation. *J Membrane Sci* 2020;611:118288. [DOI](#)
84. Zhou B, Li Q, Zhang Q, Duan J, Jin W. Sharply promoted CO₂ diffusion in a mixed matrix membrane with hierarchical supra-nanostructured porous coordination polymer filler. *J Membrane Sci* 2020;597:117772. [DOI](#)
85. Luo D, He Y, Tian J, Sessler JL, Chi X. Reversible iodine capture by nonporous adaptive crystals of a bipyridine cage. *J Am Chem Soc* 2022;144:113-7. [DOI](#) [PubMed](#)
86. Cheng K, Li H, Li Z, Li P, Zhao Y. Linking nitrogen-rich organic cages into isoreticular covalent organic frameworks for enhancing iodine adsorption capability. *ACS Mater Lett* 2023;5:1546-55. [DOI](#)
87. Cheng K, Li H, Wang JR, Li PZ, Zhao Y. From supramolecular organic cages to porous covalent organic frameworks for enhancing iodine adsorption capability by fully exposed nitrogen-rich sites. *Small* 2023;19:e2301998. [DOI](#) [PubMed](#)
88. Zhao XJ, Liu SH, Sun JK. Hierarchically porous poly(ionic liquid) - organic cage composite membrane for efficient iodine capture. *Chemistry* 2022;28:e202201199. [DOI](#) [PubMed](#)
89. Hao S, Jia Z, Wen J, et al. Progress in adsorptive membranes for separation - A review. *Sep Purif Technol* 2021;255:117772. [DOI](#)
90. Xu T, Wu B, Hou L, et al. Highly ion-permselective porous organic cage membranes with hierarchical channels. *J Am Chem Soc* 2022;144:10220-9. [DOI](#) [PubMed](#)
91. Li M, Ma J, Pan B, Wang J. Cage-based covalent organic framework for the effective and efficient removal of malachite green from wastewater. *ACS Appl Mater Interfaces* 2022;14:57180-8. [DOI](#) [PubMed](#)
92. Srivastava S, Sinha R, Roy D. Toxicological effects of malachite green. *Aquat Toxicol* 2004;66:319-29. [DOI](#) [PubMed](#)
93. Bhandari P, Mukherjee PS. Covalent organic cages in catalysis. *ACS Catal* 2023;13:6126-43. [DOI](#)
94. Sun JK, Zhan WW, Akita T, Xu Q. Toward homogenization of heterogeneous metal nanoparticle catalysts with enhanced catalytic performance: soluble porous organic cage as a stabilizer and homogenizer. *J Am Chem Soc* 2015;137:7063-6. [DOI](#) [PubMed](#)
95. Yang X, Sun J, Kitta M, Pang H, Xu Q. Encapsulating highly catalytically active metal nanoclusters inside porous organic cages. *Nat Catal* 2018;1:214-20. [DOI](#)
96. Song Q, Xu D, David Wang W, et al. Ru clusters confined in Hydrogen-bonded organic frameworks for homogeneous catalytic hydrogenation of N-heterocyclic compounds with heterogeneous recyclability. *J Catal* 2022;406:19-27. [DOI](#)
97. Zhu L, Yang X, Sun JK. Cooperative cage hybrids enabled by electrostatic marriage. *Chem Commun* 2023;59:6020-3. [DOI](#) [PubMed](#)
98. Li M, Peng Y, Yan F, et al. A cage-based covalent organic framework for drug delivery. *New J Chem* 2021;45:3343-8. [DOI](#)
99. Alimi LO, Fang F, Moosa B, Ding Y, Khashab NM. Vapor-triggered mechanical actuation in polymer composite films based on crystalline organic cages. *Angew Chem Int Ed Engl* 2022;61:e202212596. [DOI](#) [PubMed](#)
100. Han R, Wu P. Composite proton-exchange membrane with highly improved proton conductivity prepared by in situ crystallization of porous organic cage. *ACS Appl Mater Interfaces* 2018;10:18351-8. [DOI](#) [PubMed](#)
101. Liu SH, Zhou JH, Wu C, Zhang P, Cao X, Sun JK. Sub-8 nm networked cage nanofilm with tunable nanofluidic channels for adaptive sieving. *Nat Commun* 2024;15:2478. [DOI](#) [PubMed](#) [PMC](#)